Chapter 3

Results

The results section is divided into three main parts. The first part explains the experiments setting up various conditions. The next part is for the main experiments: Experiments are explained that were done with the phosphorothioate technique. The last part concerns computational analysis. In this section some data were analyzed and compared with the recent 70S X-ray crystal structure. For this purpose we mainly used the programs Ras-Mol and POV-Ray for Windows^{TM} besides some data search programs.

3.1 Setting up the Experimental Conditions

The very beginning of every new experimental project starts with the setting up conditions and checking various parameters in order to reach accurate and reliable final results. In the first part of the result section, we will present main conditions or some troublesome situations that we faced during the whole work.

3.1.1 RNase Assay: EF-Tu - an example with contamination

The experiments performed in this thesis are mainly RNA studies. While working with RNA extreme caution should be applied, even though still RNase contamination might be inevitable. The best way, then, can be checking all components of the main experiments with a sensitive RNase test.

Detection of possible RNase contamination was performed by a novel method developed in our laboratory. Details of the experimental procedure is as explained in the method part (see section 2.7.1). For this assay, MF-mRNA was, first, labeled with ^{32}P from the 5'-end and the specific activity was

adjusted to about 10,000 dpm/pmol. MF-mRNA has practical free of secondary structure. Its open conformation is a good target for any RNase attack and has provided an advantage to us to use it as a marker in our RNase assays. Generally, about 2,000 - 3,000 dpm or higher amounts of labeled mRNA were incubated with the samples of interest in a total volume of 5-10 □l. The end volume of the reaction was adjusted with H_2O. To enhance the reaction for possible RNase degradation in the case of contamination, samples were incubated at 37 ℃ for 5 min. After addit ion of RNA loading buffer and denaturing at 85-90 ℃ for 1 min, samples were loaded into a 13% polyacrylamide gel.

Using the RNase test, the buffers and other components of *in vitro* translation assay which are important for footprinting experiments were checked. Figure 3.1.1.1 is an example of the results of one of these tests. This figure shows the analysis of some of the components participating in the reactions. The lane containing MF-RNA (lane 1) is the positive control and lane13 with PK is the negative control, since it was previously shown that PK contains RNase contami-nation.

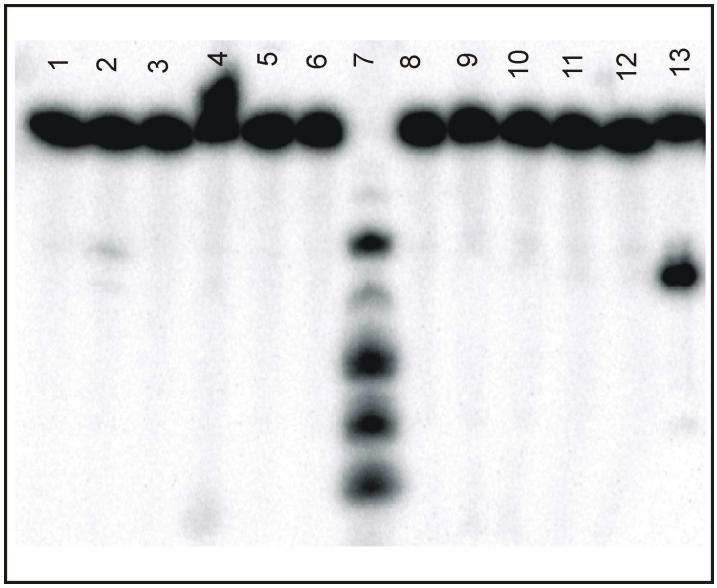

Figure 3.1.1.1: Example of a 13% AA gel for an RNase test. Some components for the Watanabe reaction: 1, MF-mRNA; 2, MFV-mRNA; 3, $tRNA^{Phe}$; 4, 70S; 5, [^{14}C]Val-$tRNA^{Val}$; 6, [^{3}H]Val-$tRNA^{Val}$; 7, EF-Tu; 8, GTP; 9, MixI; 10, MixII; 11, Tico buffer; 12, HMK; 13, PK. A reaction mixture contained 3 µl sample, 0.3 µl MF-mRNA (approximately 2,000 dpm), 2 µl H_2O and 2 µl dye.

According to this and some other experiments, we found that EF-Tu is contaminated with RNase (see Figure 3.1.1.1, lane 7). In order to understand whether this contamination was co-purified with EF-Tu or introduced afterwards, we purified EF-Tu again with the same procedure and analyzed each elution fraction of purification. C-terminal His-tagged EF-Tu was overexpressed and purified via Ni-Agarose column. Elution was done with the buffer ($T_{50}N_{50}K_{50}M_{10}SH_{10}GDP_{0.05}$) containing 80 mM imidazole. Fractions with a volume of 1ml were collected. Each elution fraction was checked for the protein by two different methods. 5 µl of each fraction was loaded to acrylamide-SDS gel and 10 µl of each was used in the spot test (Figure 3.1.1.2). In this test, 10 µl samples were put to the filter paper where the paper was marked for the fraction numbers with a pen beforehand. Coomassie staining was done to follow the fractions, which contain the protein. Fractions with protein make dark blue spots on the paper after staining in contrast to those, which do not contain the protein. Spot test results are in good agreement with the gel results (data not shown).

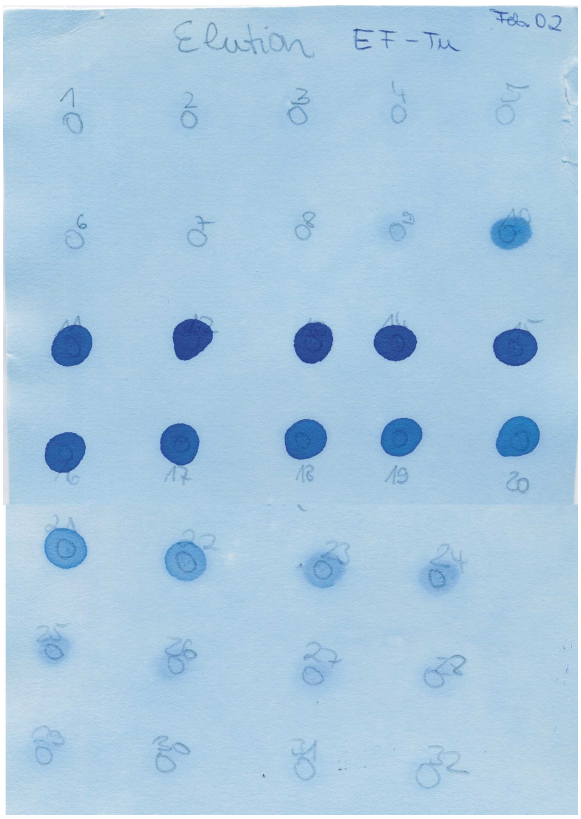

Figure 3.1.1.2: 10 µl from each of the elution fractions of the His-tagged EF-Tu were loaded to the filter paper and staining were done with coomassie blue. Dark blue spots show the main fractions containing the EF-Tu.

Figure 3.1.1.3 shows the elution profile results. We prepared individual pools with five consecutive fractions and analyzed the contamination in these pools. For example, Pool 3 contains elution fraction 11, 12, 13, 14, 15 and Pool 4

has the fraction 16, 17, 18, 19 and 20. The main reason of creating pools was to save the available material. The right panel of the figure shows the detailed analysis of pool 3 and 4 where the main EF-Tu is coming (see Figure 3.1.1.2) and marked with the red box in the left panel. Results showed that RNase contamination was due to the co-purification with EF-Tu. In order to get pure EF-Tu we needed to go one step further and do gel-filtration. Superdex 75 was used as a matrix and 150 A_{230} EF-Tu was loaded onto the column. 3 ml fractions were collected. Three main peaks were observed in A_{230} optical measurement (data was not shown). The first peak was mainly including the RNase. Blue box in Figure 3.1.1.3 shows the RNAse test of some of the fractions of the second and third peaks from the FPLC run. Fraction 51 was the main one that we used in our main experiments since it was completely free from the contamination.

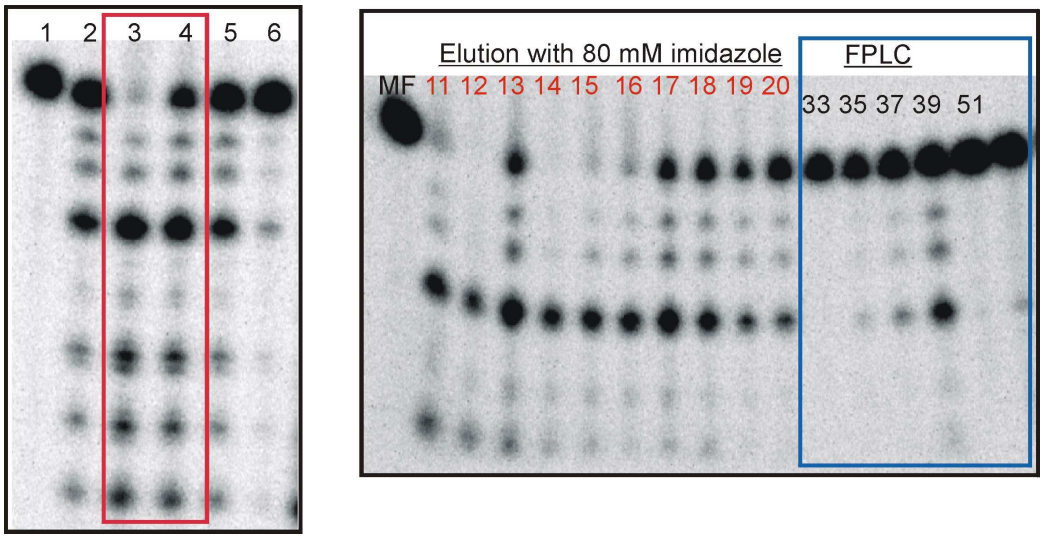

Figure 3.1.1.3: Left panel: Pools of EF-Tu fractions. Each pool contains five-elution fraction. EF-Tu mainly comes in the pool 3 and 4, which were red-boxed. Pool 3 is the combination of fractions 11-15 and pool 4 is the combination of fractions 16-20. Right panel: Detailed analysis of the fractions of pool 3 and 4 that were marked with a red box in the left panel. Right panel also includes the result of FPLC which was done .for a further purification. 33, 35, 37, 39, 51 are the elution fraction numbers from the FPLC run.

3.1.2 Poly(U): A troubleshooting against a smear problem in the footprinting experiments

The general scheme of the phosphorothioate experiments was explained in the methods part (see section 2.5.5). Following this scheme, Pi complexes were prepared, purified and cleavage experiments were done.

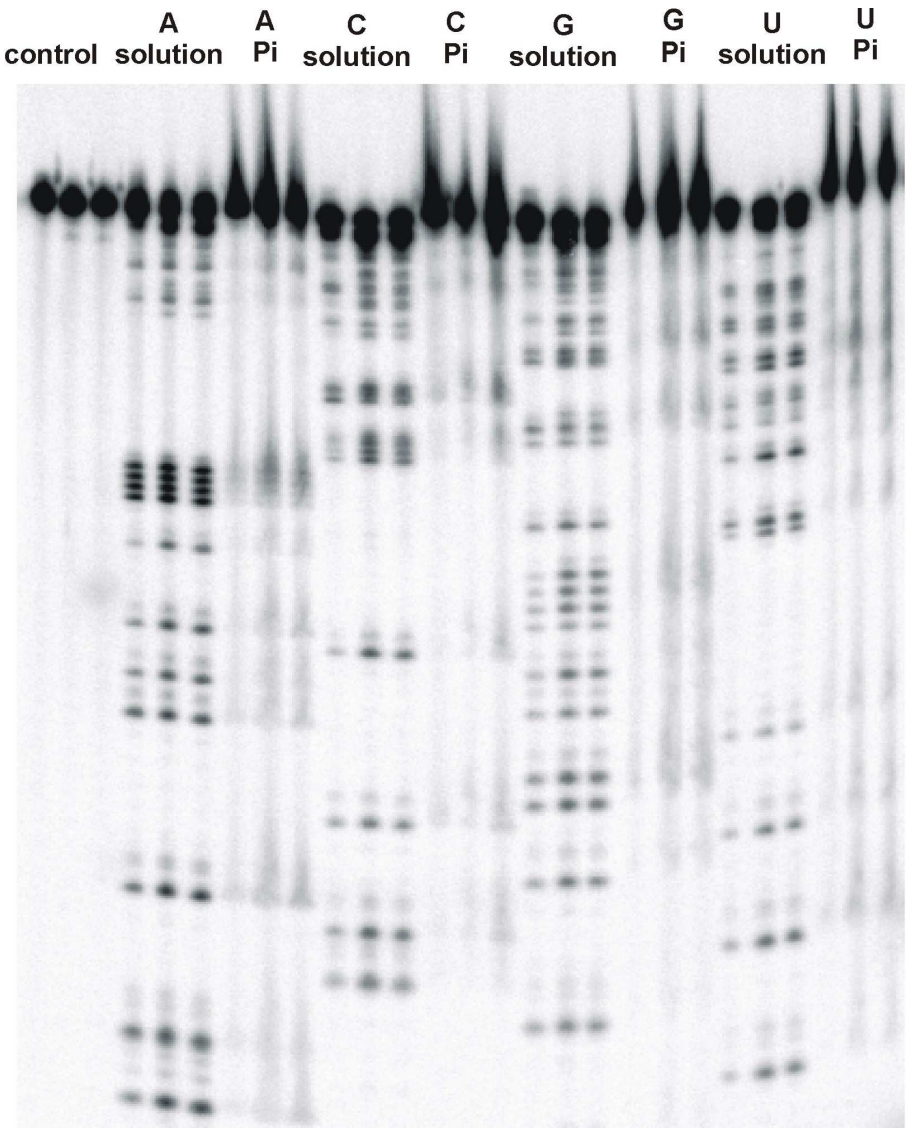

Figure 3.1.2.1: An example to the smear problem.13% AA gel for the iodine cleavage (10,000 dpm/lane). Control is the transcribed $tRNA^{Phe}$ without iodine treatment. Pi is the cleavage pattern of a $tRNA^{Phe}$ in the P site of poly(U) programmed 70S ribosome and solution means that of a tRNA cleaved in solution.

In the first experiments (see section 3.2.1), we had a lot of difficulties to get clear and sharp bands when ribosome complexes were analyzed; instead the bands were hidden in a smear (Figure 3.1.2.1), whereas tRNA in solution gave clear bands. The first possible explanation was that ribosomal proteins were not completely successfully removed before applying the extracted RNAs to the gel. Many different procedures were tried such as, different lengths shaking times in the presence of phenol and number of repetitions of phenolization, addition of different percentage of phenol or diluting the phenol with either H_2O or with binding buffer. Experiments were repeated also with Boehringer poly(U) and MF-mRNA. Clear differences in the sharpness of bands were observed in the presence of either poly(U) (smear) or MF-mRNA (no smear; Figure 3.1.2.2). A possible cause for the smear problem could be the length of the mRNA: poly(U) has more than 1000 nucleotides, whereas MF-mRNA is 46 nucleotide long and shows in footprinting experiments sharp bands. As a control, addition of poly(U) to the reaction mixture of MF-mRNA right before loading to gel turns the sharp

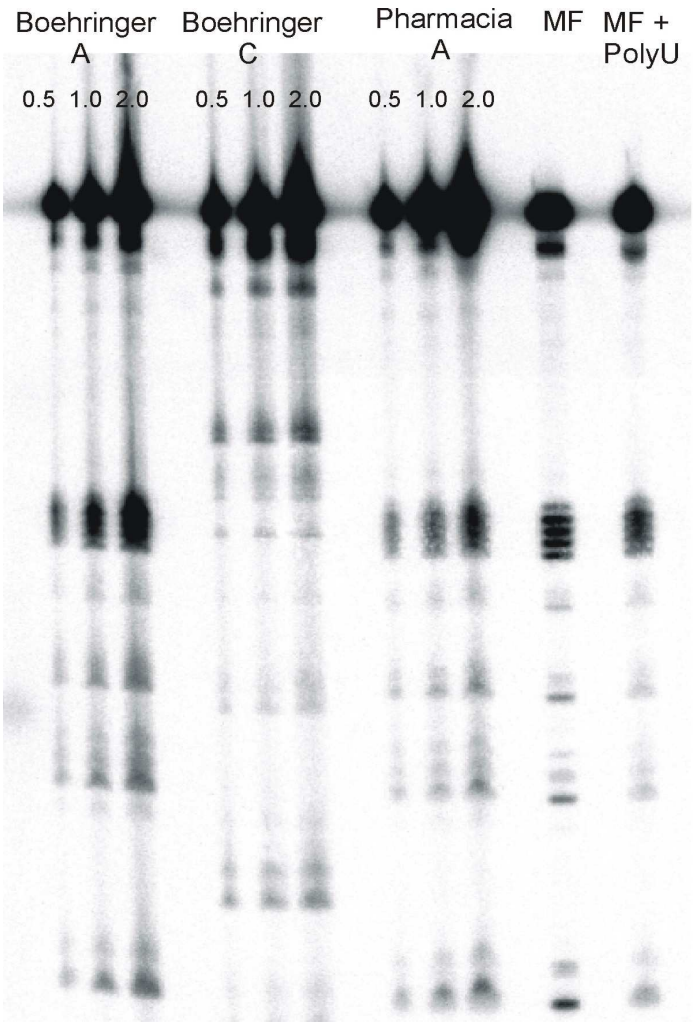

Figure 3.1.2.2: 13% AA gel for the iodine cleavage experiment. 0.5, 1.0, 2.0 are µl-amounts that were loaded to the gel. MF is the mRNA to program 70S ribosome.

bands into the smear again (Figure 3.1.2.2) indicating that simply the presence of long poly(U) mRNA are causing the smear.

Since Boehringer poly(U) has shorter chain lengths than that purchased from Pharmacia, we decided to fractionate the former one with gel filtration method (see section 2.7.2) and used the smallest fragments for our further experiments. The elution profile of poly(U) is shown in Figure 3.1.2.3A. X-axis shows the fraction numbers and Y-axis the absorption values. The highest absorption value was observed in the fraction 20, which has a 125±75-nucleotide length according to our calculations. The longer fractions have smaller absorption values showing inverse relationship between molecular weight and OD. Figure 3.1.2.3B shows the fractions on the 4% AA gel.

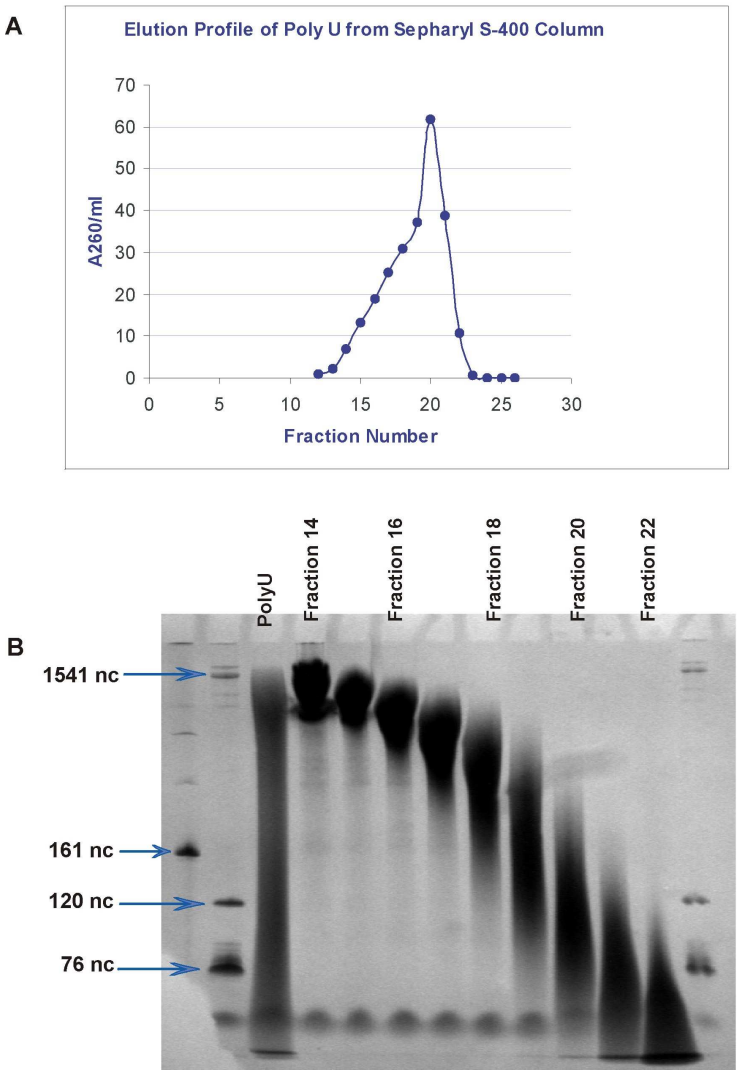

Figure 3.1.2.3: A: Elution profile of poly(U). **B:** 4% AA gel with the same OD from each fraction (1.5 A_{260}). Markers: 16S rRNA (1541 nucleotides), 5S rRNA (120 nucleotides), tRNA (76 nucleotides) and a 161 nucleotide long RNA fragment. nc: nucleotide.

Fraction 14 has the longest length and 22 has the shortest one. Lane "poly(U)" is the poly(U) before fractionation that shows clearly a population combining different lengths of fragments.

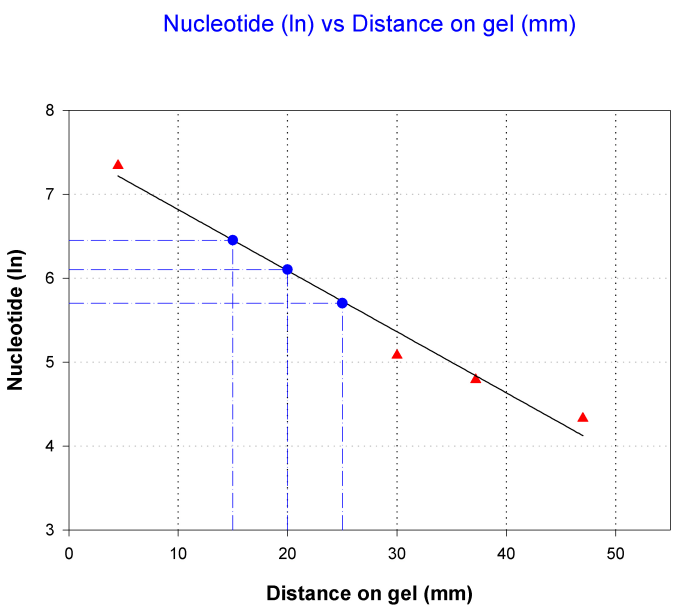

Graph 3.1.2.1: Graph nucleotide (ln) versus distance on gel (mm). Red triangles are the positions of the markers (1541, 161, 120, 76 nt) and blue is for the poly(U) fraction 18 as an example to the calculations.

As it was explained in the methods section (2.7.2) some calculations were necessary in order to find the approximate concentration of each fractions. Firstly, the distance between the markers and their loading slots on the gel was measured (Figure 3.1.2.3). The nucleotide length of each marker was converted into logarithm. A graph (nucleotide (ln) versus distance on gel) was drawn as a next step (Graph 3.1.2.1). The distance of each fraction from the slot was measured. Since it is a smear rather than one sharp band, the-mid point was chosen for the real value and the both ends of smear

Frac. No	Y-axis (ln)	Nucleotides	Estimated
14	7,4-7,24-7,08	1636-**1394**-1188	1400+/-250
15	7,24-7,08-6,92	1394-**1188**-1012,3	1200+/-200
16	7,08-6,84-6,44	1188-**934,5**-626,4	900+/-300
17	6,84-6,64-6,40	934,5-**765,1**-601,9	750+/-150
18	**6,56-6,20-5,84**	706,3-**492,8**-343,8	500+/-150
19	6,00-5,28-4,56	403,4-**196,4**-95,6	250+/-150
20	5,20-4,68-4,16	181,3-**107,8**-64,1	125+/-75
21	4,30-3,92-3,56	73,7-**50,4**-35,2	50+/-20

Table 3.1.2.1: This table is showing he each fraction and the concentration calculation of each fraction according to the Graph 3.1.2.1

were measured for the deviations. These values were plotted into the same graph (x-axis) and the corresponding y values were converted to nucleotide numbers.

In the Graph 3.1.2.1, fraction 18 is taken as an example. Three blue dots are the mid and the both ends of the fraction. The length of each fraction with the deviations and estimated values were shown in Table 3.1.2.1. In order to calculate the concentrations as pmols, we make use of the molar extinction coefficient of U, which is 1x 10^4 M^{-1} x cm^{-1}. An example of the general calculations is given below.

Example to Calculations:

Fraction 21 with 50 nucleotide; U_{coeff}= 1x10^4 $M^{-1}cm^{-1}$

50 x 1x10^4 $M^{-1}cm^{-1}$ is for a chain length with 50 nucleotides

➔ 1 mol/l gives 500 000 A_{260}/ml, this is identical to

1 µmol/µl; this value is reduced by 6 orders of magnitude yielding

1 pmol/µl with 0.5 A_{260}/ml

1A_{260} unit = 2000 pmol for 50 nucleotides

1A_{260} unit = 2000 x 50 / 125 = 800 pmol for 125 nucleotides

For the concentration calculations, each of the estimated length (Table 3.1.2.1) is multiplied by the coefficient of U. Unit of this multiplication is a large value with the dimension A_{260}/ml and equals to 1mol/l. In this way, one can easily convert the molar concentration value to an expression given as pmol/µl as shown in the example.

Next we checked the effect of the length of the poly(U) used for the preparation of an P_i complex on the sharpness of a band in the sequencing gel after an iodine induced cleavage of phosphorothioated tRNA. To this end the first Poly U fractions that was eluted (fraction number 14 and 15 with an estimated lengths 1400±250 and 1200±200 respectively) and the last two (fraction number 20 and 21 with an estimated lengths 125±75 and 50±20 respectively) were used for the preparation of Pi complexes and iodine

cleavage (Figure 3.1.2.4). The result clearly showed that the length of poly(U) was the main factor for getting smear. We decided to continue for the further experiments with the poly(U) of the fraction number 20 and 21.

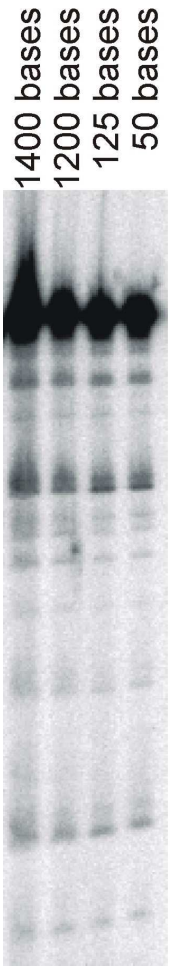

Figure 3.1.2.4: Iodine cleavage for the Pi complexes prepared with different lengths of Poly U (1400, 1200, 125, 50 bases). 10,000 dpm samples were loaded per lane.

3.1.3 Removal of unbound tRNA from ribosomal complexes

After iodine cleavage, non-bound tRNAs should be removed from the incubation mixture. For this reason we tried different gel filtration columns in order to find an acceptable separation between the ribosome and unbound tRNAs. Under the same conditions where we prepared the complexes, we mixed 3 A_{260} 30S and 10,000 dpm [^{14}C]PhetRNA^{Phe}. The main idea behind it was that since non-programmed 30S and tRNA cannot make complexes we can easily follow the separation of A_{260} material (30S) and the cpm label ([^{14}C]PhetRNA^{Phe}). Eight fractions were collected from each column and measured for radioactivity to follow tRNA and optical density to follow 30S subunits. The results are shown in Figure 3.1.3.1.

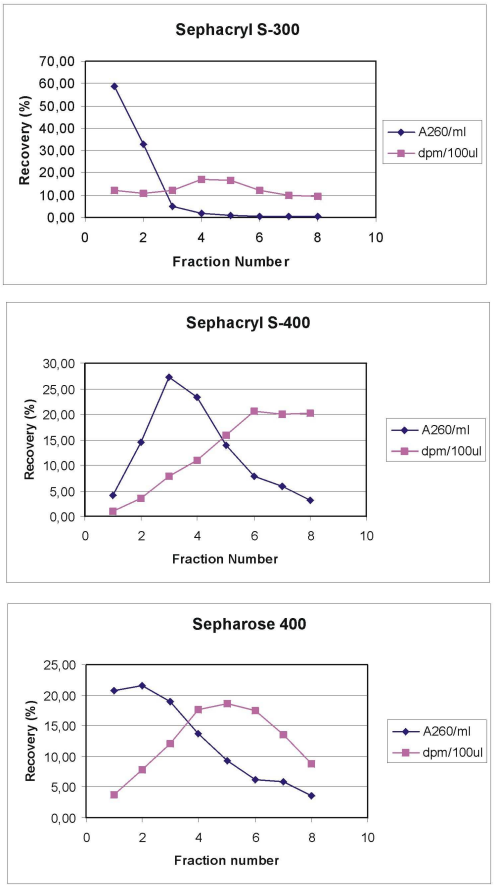

Figure 3.1.3.1: Column separation of non-programmed 30S subunits and [^{14}C]Phe-tRNA^{Phe}.

In the first fraction of each column the recovery of the 30S is changing. In the Sephacryl-300 it is roughly 60%, and below 10 % unbound tRNA is coming together. In the case of Sephacryl-400 one should collect the first three fractions to get roughly 50% recovery and the total tRNA ratio is approximately 15%. Collection of the first two fractions would give less than 10% tRNA contamination, but on the other hand the yield of 30S is not more than 20 % which is a big loss. Sepharose-400 (CL-B4) is following more or less the same pattern in the elution of tRNA as seen with Sephacryl-400. Recovery of 30S is reaching approximately 60% in the combination of the first three fractions.

We decided to use Sephacryl-300 for complex purification. This column was used in the first part of the thesis. Since the company stopped producing it during our work, we later shifted to purification via sucrose cushion (see section 2.5.5.3).

3.1.4 tRNA charging

In this project, we mainly used transcribed [^{32}P]5'-thioate-tRNA^{Phe} in the form of either deacyl-tRNA or N-acetyl-aminoacyl-tRNA. Native Ac[^{14}C]Phe-tRNA^{Phe} is used to set up the conditions. The other tRNA that was used in the oscillating ribosome experiments was the native [^{3}H]Val-tRNA^{Val}.

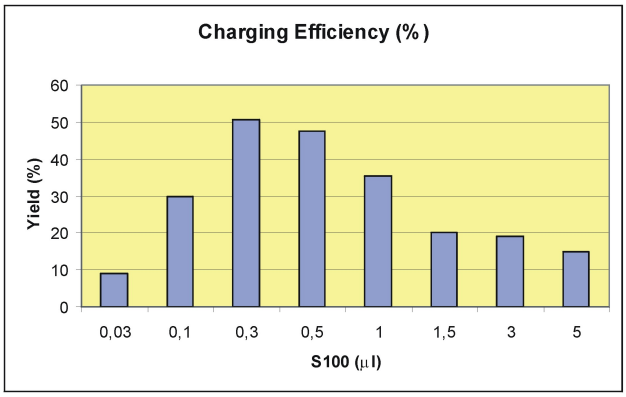

Figure 3.1.4.1: S100 titration experiment for charging [^{3}H]Val-tRNA^{Val}. The experiment was repeated three times.

For the charging of [^{3}H]Val-tRNA^{Val}, amino acid titration (3, 5, 7, 10 fold over tRNA), kinetics (5, 10, 15, 20 min) and an S100 titration were performed. 30 µl analytic charging which contains 50 pmol tRNA^{Val} was done as explained in the section 2.6.1. After incubation each sample was divided into two aliquots (2 times 14 µl) for double determination and the results were checked with cold TCA precipitation (see section 2.2.3). The optimal conditions was found as following: three molar excess of amino acid over tRNA, 0.3-0.5 µl S100 in 30 µl reaction (see Figure 3.1.4.1) and 10 min 37 $^{\circ}$C incubation time. Interesting charging efficiency behavior was observed with increasing amounts of S100. Increasing concentration of the enzyme caused a decrease in the aminoacylation, which could be due to traces of RNases of the S100 batch used for this experiment. Three times repetition of the same experiment with different S100 batches showed the same tendency. However, a corresponding S100 titration for tRNA^{Phe} charging in polyamine buffer

revealed a different behavior (see Figure 3.1.4.2), namely increasing amount of S100 had no significant effect on the charging efficiency. Therefore, RNases do not seem to provoke the effect seen with charging $tRNA^{Val}$.

For the charging efficiency of transcribed $tRNA^{Phe}$ two different buffers were checked, namely conventional buffer ($H_{50}M_{10}K_{100}SH_5$) and polyamine buffer ($H_{20}M_{4.5}N_{150}SH_4Sd_2Sp_{0.05}$). Charging was done in analytic scale (30 µl, 50 pmol tRNA per reaction) and results were determined with the cold TCA precipitation (2 times 14 µl for double determination). S100 titration experiments (0.5, 1, 2, 4, 8 and 10 µl) in two different buffers showed different results (Figure 3.1.4.2). In conventional buffer system maximum charging was about 50% in the presence of 0.5 and 1 µl enzyme. The yield was slightly decreasing with an increasing amount of S100. On the other hand, in the polyamine system the charging efficiency reached 40% in about 1 µl S-100. In both cases, native $tRNA^{Phe}$ was used as a control. The control showed the same yield in both systems with roughly 70% charging. Since the charging efficiency of transcribed tRNA is higher in the case of conventional buffer, we executed large scale charging with this buffer.

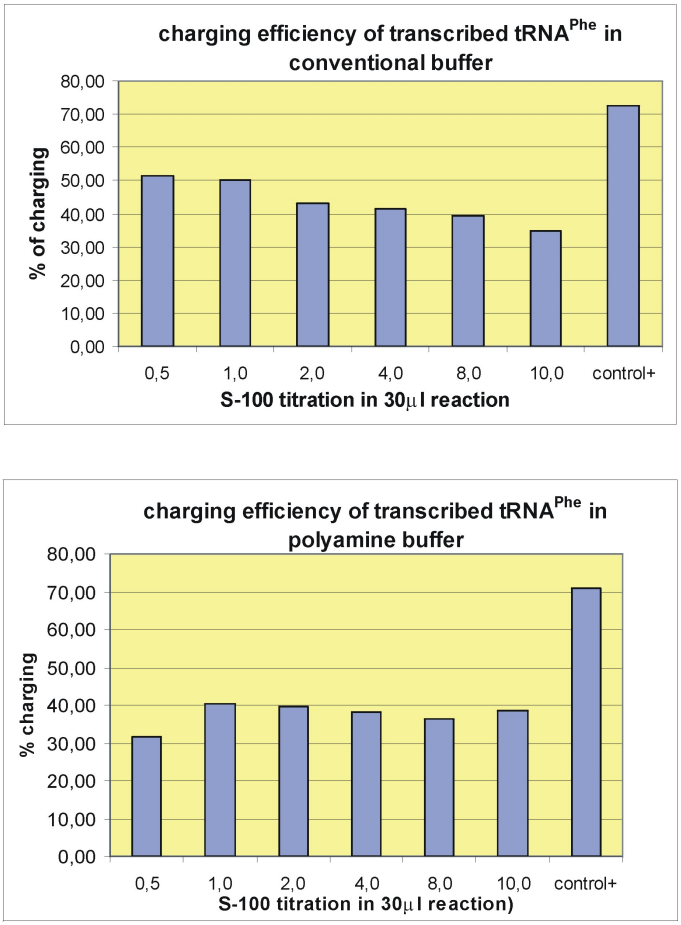

Figure 3.1.4.2: Chart for the charging efficiency of transcribed $tRNA^{Phe}$ s in two different buffers. X-axis gives the amount of S100 enzymes in the 30 µl reaction and y-axis is the yield as percentage of the input tRNA.

tRNAs that were used in the footprinting experiments have to be 5'-labeled with [γ-^{32}P]ATP in order to detect the cleavages in the sequencing gel. Generally, the order of preparing double labeled tRNA (that means 5'-^{32}P labelling and aminoacylation with the ^{14}C or ^{3}H-amino acid) sees first the 5' labelling and then the charging reaction. The disadvantage of this order is the following: since the whole procedure takes roughly two weeks for the phosphorothioated tRNAs (four thioated-tRNAs and one non-thioated tRNA should be prepared simultaneously), however when they are ready, the ^{32}P label decayed already by 50% (one half life). For this reason, we tried to set up conditions in the opposite order, namely first charging, then dephosphorylation reaction and re-phoshorylation reaction with [γ-^{32}P]ATP. However, during the dephosphorylation step the aminoacyl-tRNAs lost their amino acids due to the breakage of ester bond at the high pH conditions, which is necessary for the dephosphorylation step (data not shown). The alternative trial would be to dephosphorylate the tRNA first and then aminoacylate and re-phosphorylate. Dephosphorylation reaction was done as described in the method section (2.5.3.1) and 50 pmol dephosphorylated transcribed tRNA^{Phe}, native and transcribed tRNAs were charged in analytic scales (30 µl reaction, three molar excess of amino acid over tRNA, 15 min 37 $^{\circ}$C incubation, conventional buffer system). Surprisingly, transcribed tRNA^{Phe} and dephosphorylated one had roughly the same charging efficiency (44% and 38%, respectively; see Figure 3.1.4.3). Even though this step increased our courage to handle the whole procedure, the phosphorylation step was not

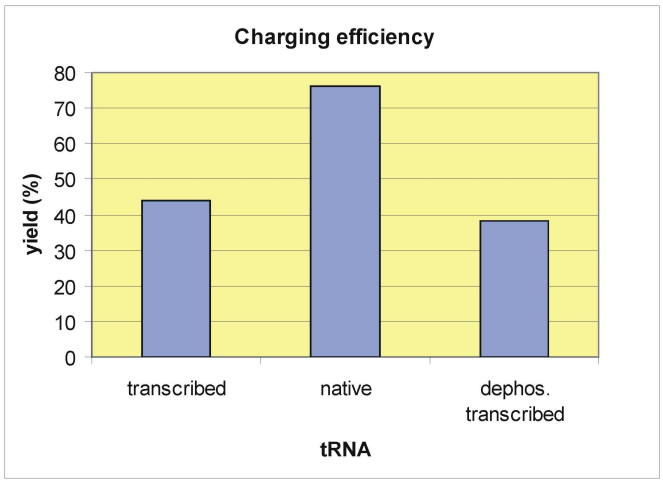

Figure 3.1.4.3: Aminoacylation efficiency of transcribed, native and 5'-dephosphorylated tRNA^{Phe}.

successful. After phosphorylation (under different pH conditions down to 6.5) samples were checked in the scintillation counter: we could not observe any ^{14}C counts for the amino acids. Samples were loaded to an acidic gel, which can separate charged and uncharged tRNAs, but a difference could not be observed (data not shown). Bands were cut from the gel and dissolved in filter count and measured. But since the ^{32}P counts were high, radioactivity separation by the scintillation counter was questionable. At this point we gave up to continue. What would be done, as a further experiment is dilution of ^{32}P-ATP with cold ATP and repeating the same experiment.

3.1.5 Dipeptide bond formation

The main idea of the experiments here was to set up experimental conditions for the dipeptide bond formation and to check the activity of some components for the phosphorothioate experiments. After couple of experiments we found ourselves in a completely different direction and in new findings. Here, we want to present some new findings and conditions for the dipeptide bond formation.

Activity control of the [^{3}H]Val-tRNA^{Val}: In order to determine the activity of the charged tRNA^{Val}, the binding efficiency and the puromycin reaction was calculated (see Figure 3.1.5.1). For these calculations, the deacyl-tRNA^{Phe} in a 2-fold molar ratio to ribosomes was bound to the P site of the MFV-mRNA programmed 70S ribosome. The re-associated 70S ribosomes were incubated in a volume of 12.5 µl with eight molar excess of the mRNA for the preparation of programmed ribosomes. The binding of [^{3}H]Val-tRNA^{Val} to the A site was done as a pre-prepared ternary complex. The ternary complex (aminoacyl-tRNA•EF-Tu•GTP) is formed immediately before its addition to the binding assay: aminoacyl-tRNA (1.5 pmol per pmol of 70S ribosomes), 0.5 mM GTP, and EF-Tu (1.5 pmol per pmol of aminoacyl-tRNA) are preincubated for 2 min at 37 ℃ under the ionic condit ions of the binding buffer and are added to the reaction mixture. Although the binding efficiency of [^{3}H]Val-tRNA^{Val} was about 60% before and after addition of the EF-G (means

in PRE and POST complexes, respectively), puromycin reaction was maximally 2-6%. Figure 3.1.5.1.1 shows one of the experimental results of these experiments.

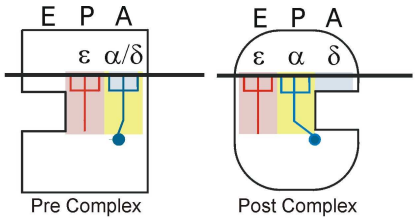

CONDITIONS:
mRNA: MFV-mRNA (8x70S)
deacyl-tRNA^{Phe} (2x70S)
EF-Tu (40 pmol/µl) (1.5xaa-tRNA)
Val-tRNA^{Val} (1.5x70S)

					BINDING							PUROMYCIN						
70S	MFV	deacyl.	Val	EF-G	dpm	dpm(av)	dpm (av)-bg	pmol/Ali	ν	PM	EF-G	dpm	dpm (av) = a	a - bdg	pmol Val-PM	%P: a(-G)/ a(+G)	%A	PM/Bdg %
-	+	+	+	-	92,5					-	-							
										+	-							
				+	82,1					+	+							
+	+	+	+	-	8783,8					-	-	113,8						
					8954,2	8869	8777	2,51	**0,63**			75	94,4					
					8154,5					+	-	120,5						
				+	8183,9	8169,2	8087	2,31	**0,58**	+	+	105,6	113,1	18,7	0,006			
												224,7						
												246,2	235,5	141,1	0,046	13,2	78	**2,0**

70S/Ali: 4 pmol
factor of filtration: 0,92
specific activity: 3801,8 dpm/pmol
factor for ethylacetate: 0,8

Figure 3.1.5.1: [^{3}H]Val-tRNA^{Val} activity test. The left part of the table shows the components that were used in the experiment, namely 70S, MFV-mRNA, deacyl-tRNA^{Phe},[^{3}H]Val-tRNA^{Val} (with a specific activity of 3802 dpm/pmol) and EF-G. Presence of the EF-G should induce the post complex. Binding test was measured by nitrocellulose filtration. Factor of filtration is 0.92 reflecting the fraction of the reaction volume applied to the filter. Puromycin reaction was done in 37 ℃, 10 min and reaction was measured with ethylacetate extraction by a factor of 0.8. The absence of 70S is for background measurement. dpm(av) is average dpm, dpm(av)-bg is the average dpm minus background. ν shows the labeled tRNA/ribosome. Puromycin reaction as a percentage was shown by PM/Bdg. %A shows the percentage of [^{3}H]Val-tRNA^{Val} in the A side after translocation and %P for the P side.

We thought that the low puromycin reaction might be either due to the puromycin activity itself or due to the low translocation efficiency because of inactive EF-G. Each of these possibilities was checked in some other assays (data not shown) and found that they were completely active. The next possibility for the low puromycin reaction was EF-Tu activity. EF-Tu might

have not formed the ternary complex or might have bound as a ternary complex but not released the ribosome thus preventing the translocation.

EF-Tu Titration: Under conventional buffer conditions with Mg^{2+} concentrations below 10 mM in the absence of polyamines, aminoacyl-tRNA binding to the A-site is EF-Tu dependent. Exploiting this fact, EF-Tu titration was performed (see Figure 3.1.5.2) by changing the concentration of the EF-Tu 0, 0.5, 1, 2, 5, 10 fold over the concentration of aminoacyl-tRNA (in this case [^{14}C]Phe-tRNA^{Phe}) which was bound to the A site. P site was pre-filled

EF-Tu fraction I

No	70S	deacyl.	aa tRNA	EF-Tu	dpm	dpm (dpm)-bg	pmol/Ali	ν
A1	-	-	+	-	37			
A2	-	-	+	10x	534			
A3	+	-	+	-	75			
A4	+	-	+	10x	483			
A5	+	+	+	-	622	139	0,11	0,02
A6	+	+	+	0.5x	2615	2132	1,65	0,33
A7	+	+	+	1x	2705	2222	1,72	0,34
A8	+	+	+	2x	2989	2506	1,94	0,39
A9	+	+	+	5x	3069	2586	2,01	0,40
A10	+	+	+	10x	3014	2531	1,96	0,39

EF-Tu fraction II

No	70S	deacyl.	aa tRNA	EF-Tu	dpm	dpm (dpm)-bg	pmol/Ali	ν
B1	-	-	+	-	38			
B2	-	-	+	10x	199			
B3	+	-	+	-	71			
B4	+	-	+	10x	177			
B5	+	+	+	-	823	646	0,50	0,10
B6	+	+	+	0.5x	1809	1632	1,27	0,25
B7	+	+	+	1x	2434	2257	1,75	0,35
B8	+	+	+	2x	2569	2392	1,86	0,37
B9	+	+	+	5x	2806	2629	2,04	0,41
B10	+	+	+	10x	2820	2643	2,05	0,41

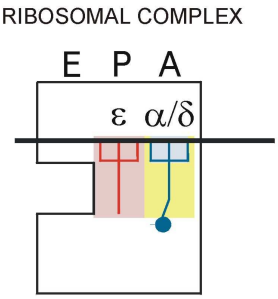

CONDITIONS:

mRNA: MF-mRNA (6x70S)
deacyl-tRNA$_f^{Met}$ (2x70S)
EF-Tu (0.5, 1.0, 2.0, 5.0, 10.0xaatRNA)
Phe-tRNA^{Phe} (0.8x70S)

Figure 3.1.5.2: EF-Tu titration under $H_{20}M_6N_{150}SH_4$, no polyamines. The binding efficiency of the [^{14}C]Phe-tRNA^{Phe} (with specific activity 1074 dpm/pmol) was checked as a ternary complex. 5 pmol 70S was used per reaction. ν shows the labeled tRNA/ribosome.

with tRNA$_f^{Met}$. Re-associated ribosomes were programmed with 6-fold excess of MF-mRNA, and the binding condition was $H_{20}M_6N_{150}SH_4$, no polyamines. Two different batches of EF-Tu fractions were checked. In both cases, in the absence of EF-Tu, aminoacyl-tRNA binding was roughly zero and the efficiency of binding increased with the increasing amount of EF-Tu. This

experiment was the indicator of active protein. Additionally, EF-Tu titration was done in the polyamine buffer system showing the same binding

EF-Tu Titration

						BINDING					PUROMYCIN							
EF-Tu over Ψ	70S	deacyl. Ψ	Phe Ψ	EF-Tu	EF-G	dpm	dpm(av)	dpm (av)-bg	pmol/Ali	ν	PM	EF-G	dpm	dpm (av) = a	a - bdg	pmol Phe-PM	%P: a(-G)/ a(+G)	%A	PM/Bdg %
	+	+	+	+							-	-	61,5 62,2	62	0	0			
1X						802,7							57						
					-	909,6	856,15		0,87	**0,29**	+	-	58,2	58	-4	-0,007			
						692,7							116,3						
					+	744,8	718,75		0,73	**0,24**	+	+	119,5	118	56	0,087	-7,58	108	**11,96**
						1637,4							40,3						
2X					-	1616,9	1627,15		1,65	**0,55**	+	-	45,9	43	-19	-0,029			
						1175,3							227						
					+	1347,6	1261,45		1,28	**0,43**	+	+	227,5	227	165	0,257	-11,3	111	**20,10**
						910,6							89,4						
5X					-	1098,3	1004,45		1,02	**0,34**	+	-	90,6	90	28	0,044			
						1057							203,2						
					+	1097,5	1077,25		1,09	**0,36**	+	+	191,2	197	135	0,21	20,8		**19,27**
						1760							64,6						
10X					-	2047,4	1903,7		1,93	**0,64**	+	-	56,1	60	-2	-0,002			
						1704,9							263,4						
					+	1375,9	1540,4		1,56	**0,52**	+	+	306,4	285	223	0,346	-0,67	101	**22,20**

70S/Ali: 3 pmol
factor of filtration: 0,92
specific activity: 1074 dpm/pmol
factor for ethylacetate: 0,6

Figure 3.1.5.3: EF-Tu titration under polyamine binding buffer conditions. dpm(av) is average dpm, dpm(av)-bg is the average dpm minus background. ν shows the labeled tRNA/ribosome. The extent of the puromycin reaction is shown as a percentage of the binding reaction.

efficiency. Puromycin reaction was already saturated (19.27%) in a 2-fold excess of the protein under polyamine buffer conditions (Figure 3.1.5.3).

Translocation efficiency in the presence and absence of EF-Tu: As a next step, two different complexes were prepared and the binding and puromycin reactions were measured in the presence and absence of EF-Tu. The first complex was a Pi complex, namely an aminoacyl-tRNA is in the P-site. This complex was prepared as a control. The second one contained a deacyl-tRNA in the P site and an aminoacyl-tRNA in the A-site. In both cases, the re-associated 70S ribosomes were incubated in a volume of 12.5 µl with an 8 molar excess of MF-mRNA. Either [^{14}C]Phe-tRNA^{Phe} (Complex 1), or deacyl-tRNA$_f^{Met}$ (Complex 2) with a 2 fold molar ratio to ribosomes were bound to the P site of the MF-mRNA programmed 70S ribosome. The binding of the

[^{14}C]Phe-tRNA^{Phe} to the A site in complex 2 was performed in the absence or presence of EF-Tu. In the presence of EF-Tu, the ternary complex (aminoacyl-tRNA•EF-Tu•GTP) was formed immediately before its addition to the binding assay: aminoacyl-tRNA (2 pmol per pmol of 70S ribosomes), 0.5 mM GTP, and EF-Tu (10 pmol per pmol of aminoacly-tRNA) was preincubated for 2 min at 37 ℃ under the ionic condit ions of the polyamine binding buffer before addition to the reaction mixture. In both cases, the background of [^{14}C]Phe-tRNA^{Phe} presence on the filter was determined in the absence of ribosome (Figure 3.1.5.4). Even though the binding efficiency of the [^{14}C]Phe-tRNA^{Phe} was around 40% in the P or A site, puromycin reaction efficiency was drastically changing from complex 1 to complex 2 and also in the presence and absence of EF-Tu (see Figure 3.1.5.4). Here we showed that when deacyl-tRNA is in the P site and aminoacyl-tRNA in the A-site, translocation is EF-Tu dependent. Even though the binding efficiency of aminoacyl-tRNA is the same in the presence or absence of EF-Tu, puromycin reaction efficiency is decreasing with a factor of 5 in the absence of EF-Tu.

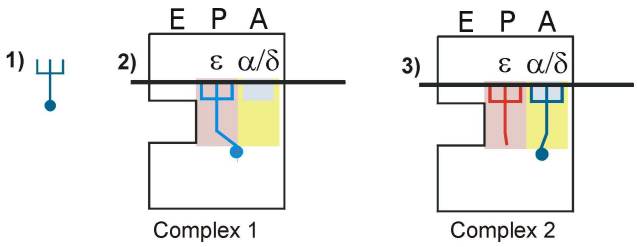

CONDITIONS:
mRNA: MF-mRNA (8x70S)
deacyl-$tRNA_f^{Met}$ (2x70S)
EF-Tu (10 x aatRNA)
Phe-tRNA (2x70S)

with EF-Tu — **BINDING** — **PUROMYCIN**

No	70S	deacyl.	Phe	EF-G	dpm	dpm(av)	dpm (av)-bg	pmol/Ali	ν	PM	EF-G	dpm	dpm (av) = a	a - bdg	pmol Ac-PM	%P: a(-G)/ a(+G)	%A	PM/Bdg %
1	-	-	+	-	179 200	189,5												
2	+	-	+	-	2347 2100	2223,5	2034	2,06	**0,41**	-	-	273 258	265,5					
										+	-	2027 2167	2097,0	1831,5	2,132			
				+	2239 1898	2068,5	1879	1,90	**0,38**	+	+	2115 2036	2075,5	1810,0	2,107	101,2	-1,2	**110,8**
3	+	+	+	-	2414 2293	2353,5	2164	2,19	**0,44**	-	-	166 194	180,0					
										+	-	305 273	289,0	109,0	0,127			
				+	2131 2124	2127,5	1938	1,96	**0,39**	+	+	802 781	791,5	611,5	0,712	17,8	82,2	**36,3**

no EF-Tu — **BINDING** — **PUROMYCIN**

No	70S	deacyl.	Phe	EF-G	dpm	dpm(av)	dpm (av)-bg	pmol/Ali	ν	PM	EF-G	dpm	dpm (av) = a	a - bdg	pmol Ac-PM	%P: a(-G)/ a(+G)	%A	PM/Bdg %
1	-	-	+	-	93 57	75												
2	+	-	+	-	1557 1598	1577,5	1503	1,52	**0,30**	-	-	155 145	150,0					
										+	-	1424 1446	1435,0	1285,0	1,496			
				+	1633 1619	1626	1551	1,57	**0,31**	+	+	1306 1359	1332,5	1182,5	1,376	108,7	-8,7	**87,7**
3	+	+	+	-	2141 2029	2085	2010	2,03	**0,41**	-	-	118 130	124,0					
										+	-	214 274	244,0	120,0	0,14			
				+	1909 1939	1924	1849	1,87	**0,37**	+	+	242 245	243,5	119,5	0,139	100,4	-0,4	**7,4**

Figure 3.1.5.4: The binding and puromycin reaction efficiency in the presence and absence of the EF-Tu. The left part of the table shows the components in the experiment, namely 70S, deacyl-$tRNA_f^{Met}$, [^{14}C]Phe-$tRNA^{Phe}$ (with a specific activity of 1074 dpm/pmol) and EF-G. Binding was measured by nitrocellulose filtration. Factor of filtration is 0.92 reflecting the fraction of the reaction volume applied to the filter. Puromycin reaction was performed at 37 ℃ for 10 min and the formed AcPhe-puromycin was extracted by ethylacetate by a factor of 0.8. The absence of 70S gives the background. dpm(av) is average dpm, dpm(av)-bg is the average dpm minus background. ν shows the labeled tRNA/ribosome. The extent of puromycin reaction is shown as a percentage of the binding value (PM/Bdg). %A shows the percentage of [^{14}C]Phe-$tRNA^{Phe}$ in the A site after translocation.

Pi site binding with different aminoacyl-tRNAs: Is there an influence of the type of tRNA on binding to the P site and the efficiency of the puromycin reaction? To this end we decided to compare the binding and puromycin reaction efficiency with different aminoacyl-tRNAs in the P site of the ribosome. For this purpose, [^{14}C]Phe-tRNA^{Phe} , [^{3}H]Val-tRNA^{Val} and Ac[^{14}C]Phe-tRNA^{Phe} were used. Results are presented in Figure.3.1.5.5.

					BINDING					PUROMYCIN							
No	70S	deacyl	**Phe**	EF-G	dpm	dpm(av)	dpm (av)-bg	pmol/Al i	v	PM	EF-G	dpm	dpm (av) = a	a - bdg	pmol Ac-PM	%P: a(-G)/ a(+G)	%A	PM/Bdg %
1	-	-	+	-			0											
2	+	-	+	-	892 1130	1010,95	1011	1,02	**0,34**	-	-	85,6 97,4	91,5					
										+	-	504,3 484,2	494,3	402,8	0,469			
				+	1095	1095	1095	1,11	**0,37**	+	+	443,1 467,9	455,5	364,0	0,424	110,6	-10,6	**38,2**

No	70S	deacyl.	**Ac**	EF-G	dpm	dpm(av)	dpm (av)-bg	pmol/Al i	v	PM	EF-G	dpm	dpm (av) = a	a - bdg	pmol Ac-PM	%P: a(-G)/ a(+G)	%A	PM/Bdg %
1	-	-	+	-	37,6													
2	+	-	+	-	1181	1181	1181	1,27	**0,42**	-	-	169,3 154,4	161,9					
										+	-	1290,4 1158,4	1224,4	1116,8	1,385			
				+	1278	1278	1278	1,38	**0,46**	+	+	1289,6 1293,4	1291,5	1183,9	1,468	94,3	5,7	**106,5**

No	70S	deacyl.	**Val**	EF-G	dpm	dpm(av)	dpm (av)-bg	pmol/Al i	v	PM	EF-G	dpm	dpm (av) = a	a - bdg	pmol Ac-PM	%P: a(-G)/ a(+G)	%A	PM/Bdg %
1	-	-	+	-	81,6													
2	+	-	+	-	2975,1 2581,9	2778,5	2779	0,79	**0,26**	-	-	214,2 220,3	217,3					
										+	-	160,2 193,2	176,7	69,1	0,023			
				+	2226,2 2409	2317,8	2236	0,64	**0,21**	+	+	192 216,9	204,5	96,8	0,032	71,3	28,7	**5,0**

Figure 3.1.5.5: Pi site binding of various tRNAs. Phe, Phe-tRNA; Ac, AcPhe-tRNA; Val, Val-tRNA. The specific activities were 1074, 1008, 3802 dpm/pmol for Phe-tRNA^{Phe}, AcPhe-tRNA^{Phe}, Val-tRNA^{Val}, respectively.

Experiments were repeated two times and gave similar results. The highest puromycin reaction was observed, when acetylated aminoacyl-tRNA is in the P site (100%). Interestingly, we could not get 100% puromycin reaction with [^{14}C]Phe-tRNA^{Phe} as we got in previous experiments (see Figure 3.1.5.4). It is likely that by mistake Ac[^{14}C]Phe-tRNA^{Phe} instead of Phe-tRNA was used in the previous experiment for binding to the P site (P_i formation). Even if so, it

does not change our conclusions in that section. Here experiments showed that aminoacyl-tRNA-puromycin reactions are not as efficient as acetylated aminoacyl-tRNA in the puromycin reaction. An extreme case is seen with Val-tRNA, where a puromycin reaction near background was observed. This experiment was repeated and since it showed the same tendency, it is reproducible.

Dipeptide bond formation: The experiments in Figure 3.1.5.4. showed that translocation efficiency with the deacyl-tRNA in the P site and ternary complex bound to the A site is low, whereas an aminoacyl-tRNA bound non-enzymatically (i.e. without EF-Tu) to the A site practically cannot be translocated. When we bind Phe-tRNA to the Pi site, puromycin reaction efficiency was significantly increased. The highest yield was obtained with the acetyl-aminoacyl-tRNA. As a next step we wanted to check complexes which were prepared with acetyl-aminoacyl tRNA in the P side instead of deacyl-tRNA. These complexes are very important for the oscillating ribosome experiments as well. Ac[^{14}C]Phe-tRNA^{Phe} added in a 2 fold molar ratio to ribosomes was bound to the P site of MFV-mRNA programmed 70S ribosome. Re-associated 70S ribosomes were incubated in a volume of 12.5 µl with 6 molar excess of mRNA for the preparation. Binding of the [^{3}H]Val-tRNA^{Val} to the A site was done as a pre-prepared ternary complex. The ternary complex (aminoacyl-tRNA•EF-Tu•GTP) is formed immediately before its addition to the binding assay: aminoacyl-tRNA (1.5 pmol per pmol of 70S ribosomes, 0.5 mM GTP, and EF-Tu with 2 pmol per pmol of aminoacly-tRNA were preincubated for 2 min at 37 ℃ under the ionic conditions of the binding buffer and are added to the reaction mixture (Figure 3.1.5.6.). The total reaction mixture was then incubated for 4 minutes at 20 ℃. The binding efficiency of Ac[^{14}C]Phe-tRNA^{Phe} was about 60% in the P site and so it was for [^{3}H]Val-tRNA^{Val} in the A site. The results also showed that even though [^{3}H]Val-tRNA^{Val} seems to be a very poor substrate for the puromycin reaction after the translocation of the Pre complex with a deacyl-tRNA in the P site and a [^{3}H]Val-tRNA^{Val} in the A site, it gives roughly 100% puromycin reaction efficiency when the complex was prepared with the acetyl-aminoacyl tRNA in the P side instead of deacyl-tRNA.

BINDING

AcPhe Binding **Val Binding**

No	70S	Ac	Val	EF-G	dpm	dpm(av)	dpm (av)-bg	pmol/Ali	v	val	Ac	EF-G	dpm	dpm(av)	dpm (av)-bg	pmol/Ali	v
Pi	+	+	-	-	2315 2223	2269,0		2,4	**0,82**								
				+	2450 2218	2334,2		2,5	**0,84**								
	+	+	+	-	1788 1812	1800,2		1,9	**0,65**	+	+	-	6291 5947,9	6119,5		1,7	**0,58**
				+	1689	1688,9		1,8	**0,61**			+	5826,7	5826,7		1,7	**0,56**

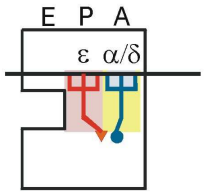

PUROMYCIN

AcPhe **Val**

No	PM	EF-G	dpm	dpm (av) = a	a - bdg	pmol Ac-PM	%P: a(-G)/ a(+G)	%A	PM/Bdg %	PM	EF-G	dpm	dpm (av) = a	a - bdg	pmol Ac-PM	%P: a(-G)/ a(+G)	%A	PM/Bdg %
Pi	-	-	217,9 215,9	216,9														
	+	-	2679,2 2289,8	2484,5	2267,6	2,81												
	+	+	2718,4 2819,1	2768,8	2551,9	3,16	88,9	11,1	**125,7**									
	-	-	269,2 248,7	259,0						-	-	170,8 129,9	150					
	+	-	1714,2 1811,3	1762,8	1503,8	1,86				+	-	2949,7 3031,6	2991	2840	0,93			
	+	+	2852 2305	2578,5	2319,6	2,88	64,8	35,2	**157,9**	+	+	5386,3 4985,3	5186	5035	1,66	56,4		**99,4**

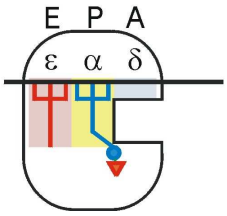

Figure 3.1.5.6: Dipeptide bond formation. The upper panel shows the binding results. Pi complex were prepared with Ac[^{14}C]Phe-tRNA^{Phe} on the P site. The lower panel is for the puromycin reaction. The absence of 70S is for background measurement. dpm(av) is average dpm, dpm(av)-bg is the average dpm minus background. ν shows the labeled tRNA/ribosome. Puromycin reaction as a percentage was shown by PM/Bdg. %P shows the percentage of [^{3}H]Val-tRNA^{Val} in the P side after translocation.

After this experiment we optimized the last step in the dipeptide bond formation experiments. The results presented in Figure 3.1.5.6 were showing that even in the case of equimolar binding of AcPhe- and Val-tRNA, an overreaction of AcPhe-tRNA exists in contrast to the reaction of Val-tRNA (158% AcPhe- and 99.4% Val-puromycin reaction). We do not see a simple explanation for this finding.

Another point of this experiment regards the fact that there was only a 40% increase in the puromycin reaction upon EF-G addition, 60% reacted already without EF-G. This finding means that most of the ribosomes were already in the POST state before the addition of EF-G. A possible reason for this is the puromycin reaction after translocation. The binding reaction of the ternary complex was performed at 20 ℃ for less than 4 min, a co ndition that prevents sliding of the formed dipeptide at the A site. However, the subsequent translocation reaction ± EF-G saw an incubation at 37 ℃ for 15 min. This condition can provoke significant spontaneous translocation, i.e. a translocation reaction in the absence of EF-G (Bergemann and Nierhaus, 1983).

Generally, all these experimental results show us that translocation efficiency with the deacyl-tRNA in the P site and aminoacyl-tRNA in the A-site is poor. We are planning further experiments for this new finding to get more data to test and enhance our observation. For this purpose we are cloning different tRNAs to check same complexes with different tRNAs in a similar manner.

3.2 Footprinting Experiments

In this part of the result section, footprinting experiments with the phosphorothioate cleavage method will be presented. We divided this part into the four subsections.

1. General overlook to the phosphorothioate experiments
2. Importance of buffer conditions.

3. Effects of mRNA on the protection pattern of the P-site bound tRNA.
4. Ribosomes oscillating between the PRE and the POST states.
   i. Puromycin reaction with the P-site bound AcPhe-tRNA^{Phe}.
   ii. Dipeptide formation

3.2.1 General overlook to the phosphorothioate cleavage experiments

Phosphorothioate method is one of the important footprinting techniques to assess the contact patterns of RNAs within ribonucleoprotein complexes. The method is based on the fact that small and chemically inert iodine (I_2) molecule can cleave the phosphate-sugar backbone of phosphorothioated RNA. Phosphorothioated RNA has a sulphur atom instead of a non-bridging O_2 at the phosphate group. The main steps of transcription yielding phosphoro-thioated tRNAs are the same as those of normal transcription assays. The thioation of the tRNA at the A, C, G, or U positions, respectively, is obtained by replacing a certain amount of the nucleotide of interest in the reaction with the corresponding [αS]-NTP. There are 15 A, 21 C, 24 G and 16 U nucleotides in the *E. coli* tRNA^{Phe}. For the transcription with theoretically 1.3 to 1.5 thioated nucleotide per tRNA (thinking that incorporation will be less and we mostly obtain tRNAs with one thioated nucleotide per molecule), we mix in tube A 0.37 mM [αS]-ATP with 3.38 mM ATP to obtain 3.75 mM total ATP, the other NTPs present (CTP, GTP and ATP) have the concentration of each 3.75 mM. Similarly, tube C contains 0.27 mM, tube G 0.24 mM, and tube U 0.35 mM [αS]-CTP, [αS]-GTP, [αS]-UTP

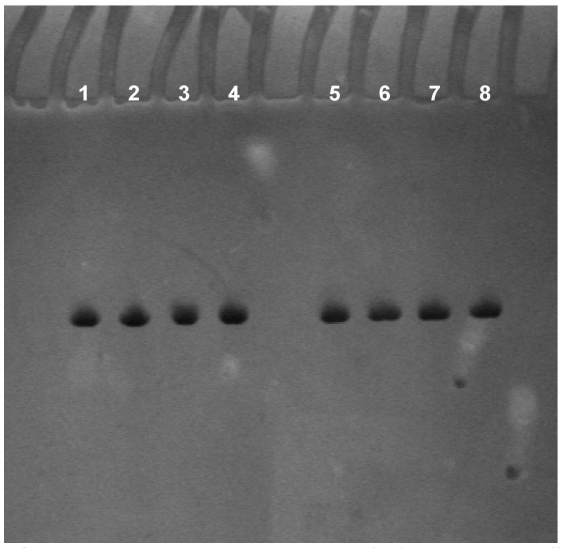

Figure 3.2.1.1: 13% AA gel for an *E.coli* tRNA^{Phe} transcription. 1-4 are the markers (transcriptions done before) for the tRNAs which contain [αS]-A, C, G, UTP nucleotides, respectively. Lanes 5-8 are freshly transcribed phosphorothioated tRNA^{Phe} in the same order.

respectively, being complemented with the corresponding un-modifed NTP to 3.75 mM in addition to the three other NTP's.

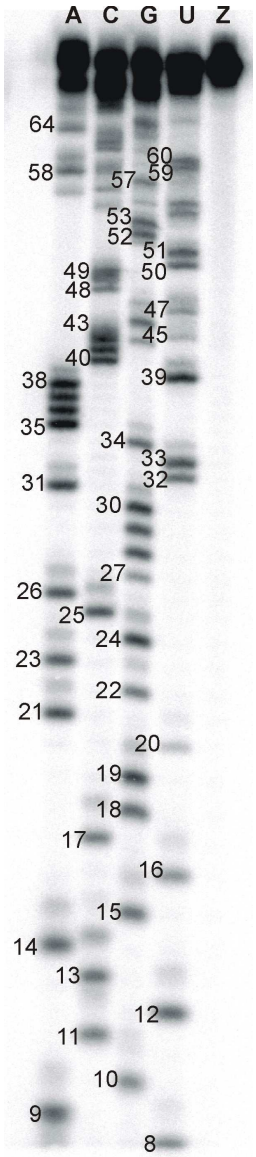

Figure 3.2.1.2: Thioated $tRNA^{Phe}$ sequencing with iodine cleavage in solution.

Usually replacement of an oxygen atom with a sulfur atom does not affect the functional spectrum of a molecule, because (i) the negative charge of the phosphate group is retained and (ii) also the size of the sulfur atom is only slightly larger than the O_2 atom. Thioated tRNA transcripts have been shown to be active in aminoacylation, ternary complex formation, and poly(Phe) synthesis (Dabrowski et al., 1995). The investigation of the protection patterns of tRNAs bound to the ribosome can be performed for all defined states of the ribosomal-binding sites. Generally, [^{32}P]5'-thioate-tRNA is bound to the site chosen for investigation. It is very important to perform control reactions, where the tRNA is free in solution. Figure 3.2.1.2 is an example gel for the iodine cleavage of $tRNA^{Phe}$ in the solution. The tRNAs are exposed to iodone (I_2) in five separate test tubes, since in four cases only one of the nucleotide was supplemented with the corresponding [αS]-NTP. For example, in figure 3.2.1.2, A shows the $tRNA^{Phe}$ with the [αS]-ATP and so on. Z is the control tRNA which does not contain any thioated nucleotide. Iodine exposure of this tRNA does not give any band.

For the oscillating ribosome experiments we had to prepare Ac[^{14}C]Phe-[^{32}P]$tRNA^{Phe}$. Preparation of the double-labeled tRNA is described in the method section (sections 2.5.3, 2.6.1). Here the HPLC results will be discussed. After charging reactions and before HPLC the double-labeled tRNAs were passed through a NAP^5 column. These fractions, each with a volume of 500 µl, were combined and directly

loaded to the HPLC after decreasing the volume in speed-vacuum centrifuge (SpeedVac) up to 500 µl.

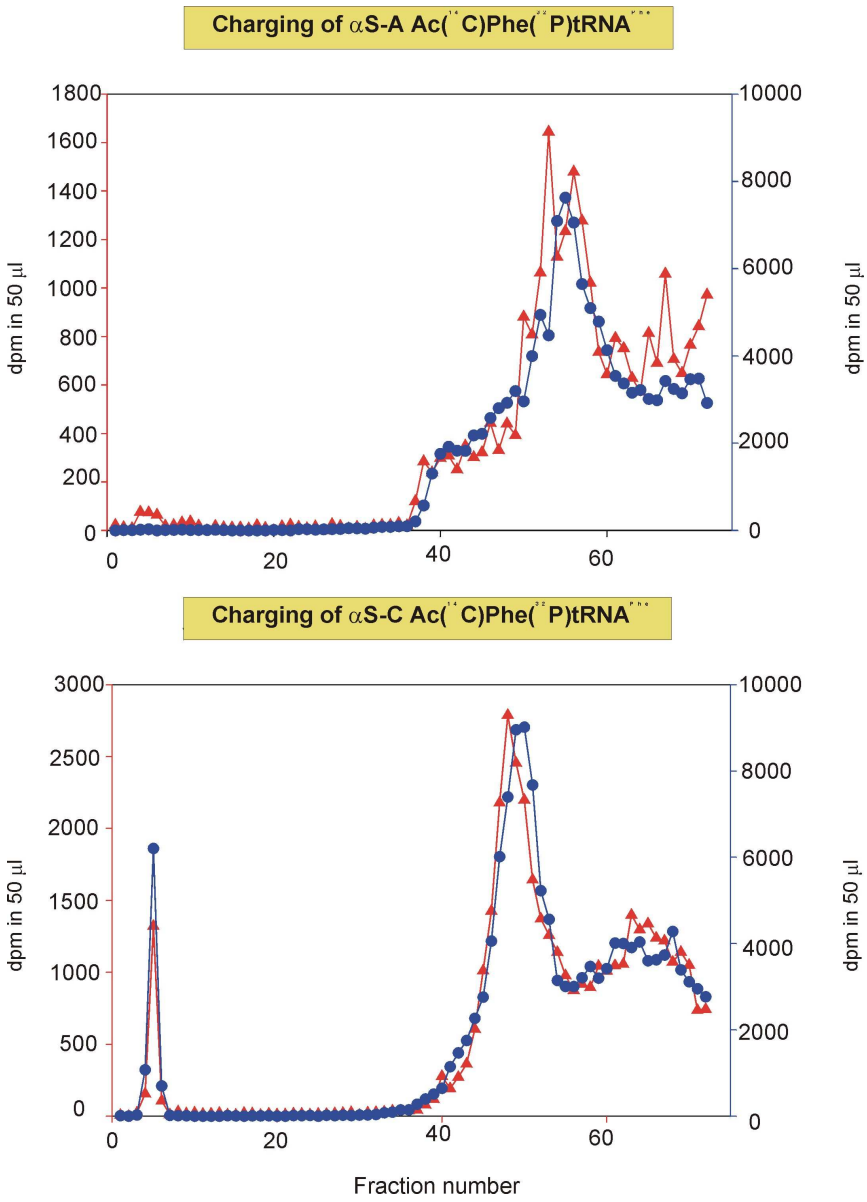

Figure 3.2.1.3a: HPLC elution profile for thioated tRNAs. Red stands for the ^{14}C counts and blue for the ^{32}P counts.

Figures 3.2.1.3a and 3.2.1.3b show the HPLC results of the 4 tRNAs. 1 ml fractions were collected (total 80 fractions from each run) and 50 µl from each fraction were measured in the scintillation counter for both radioactive isotopes (^{14}C and ^{32}P) and the graphics (fraction number versus radioactivity) were drawn.

In order to purify double labeled tRNAs (αS-N Ac[^{14}C]Phe-[^{32}P]tRNA^{Phe}), fractions which contain both radioactivity in equal molar ratios were selected For αS-A; fractions 51 to 60 (except 53 since there was huge deviation

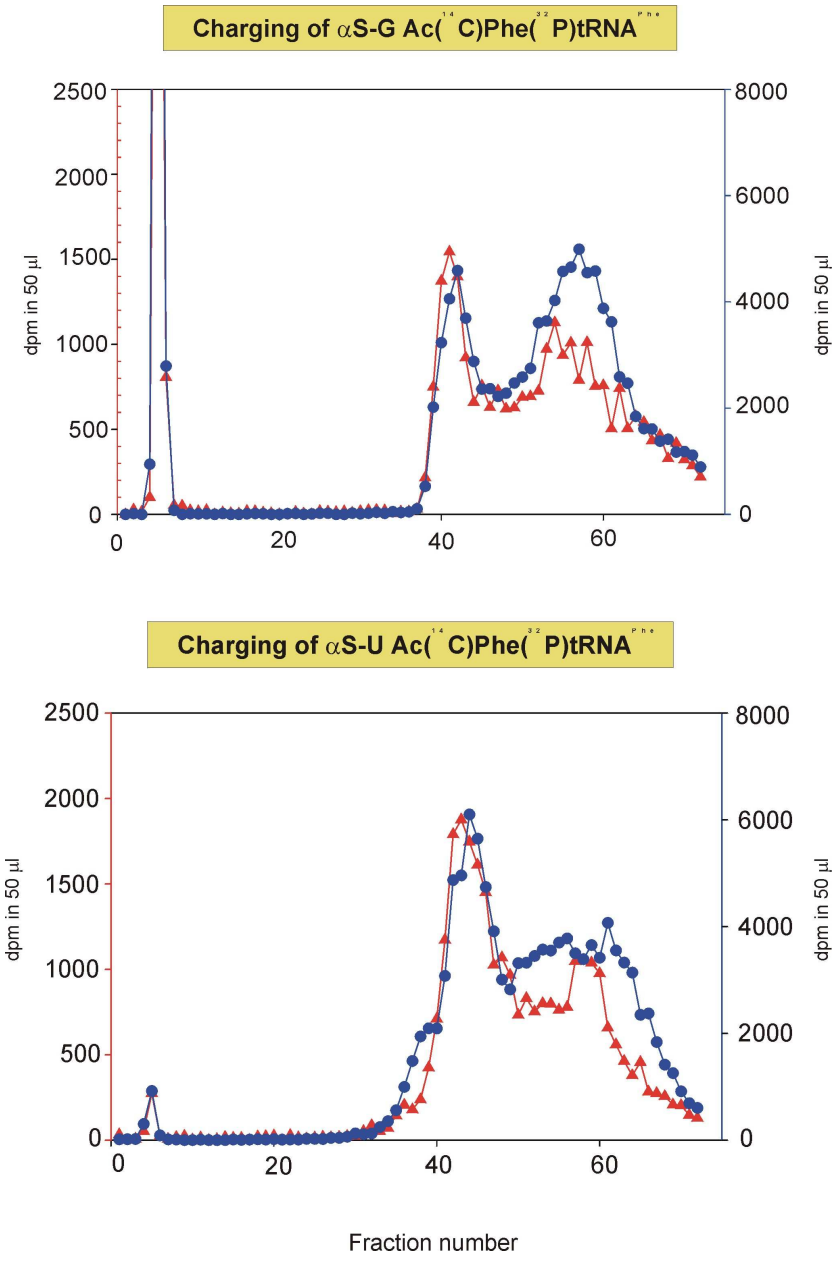

Figure 3.2.1.3b: HPLC elution profile for thioated tRNAs. Red is for the ^{14}C counts and blue is for the ^{32}P counts.

between two radioactivity amounts), for αS-C; 45 to 49 and 52 to 55, for αS-G; 38 to 45 and αS-U; 40 to 49 were collected. Combined fractions were EtOH precipitated, washed in 70% EtOH and pellets dissolved in 250 µl .

3.2.2 The protection pattern of a tRNA bound to the P site of a 70S ribosome is not significantly affected by changes in buffer composition

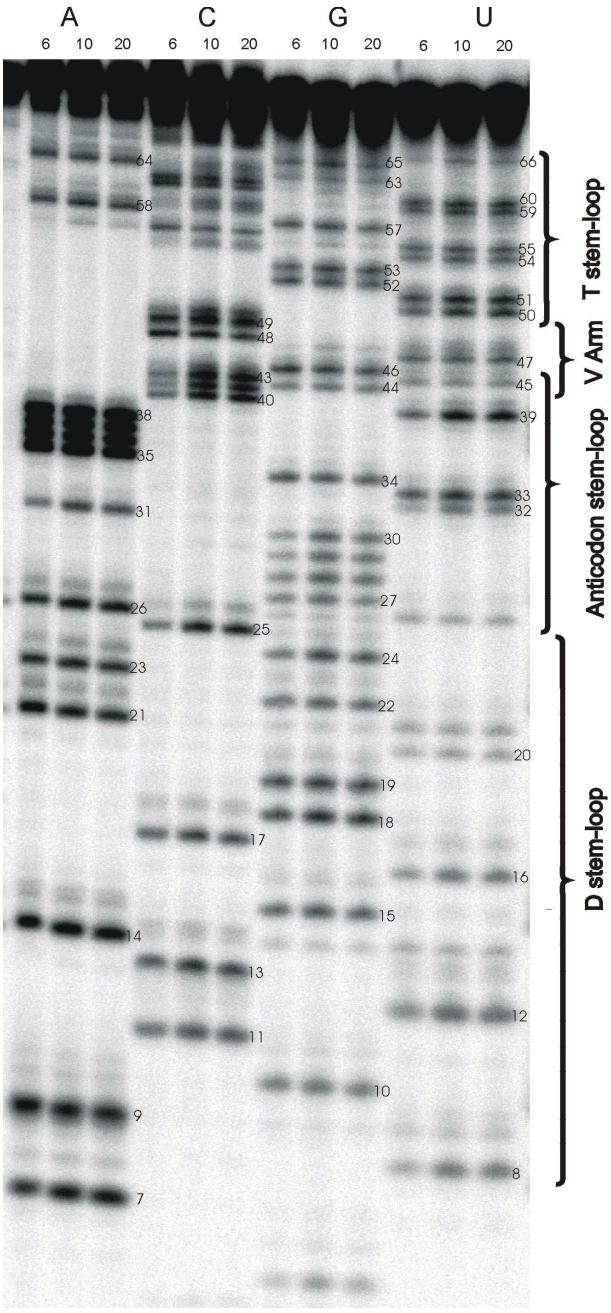

Figure 3.2.2.1: Sequencing gel of protection experiments with thioated $tRNA^{Phe}$. $tRNA^{Phe}$ was either in a buffer containing 6 mM Mg^{2+} and polyamines or in conventional buffers with 10 and 20 mM Mg^{2+} without polyamines (lanes marked with 6, 10 and 20, respectively). The numbers next to the bands indicate the nucleotide positions, structural elements of the tRNA are indicated on the right-hand side.

tRNA locations on the ribosome is highly sensitive to buffer conditions (see Discussion for details).

Based on this observation, we were interested to test whether there is a significant difference in the protection patterns of a deacylated tRNA, free in the solution and bound to the ribosomal P site, under polyamine or conventional buffer conditions.

In Solution

Figure 3.2.2.1 shows a representative footprinting gel for a deacylated $tRNA^{Phe}$ in solution under different buffer conditions. We have chosen a polyamine system that allows quantitative occupation of the tRNA binding sites at Mg^{2+} concentrations below 10 mM and protein synthesis

with a performance similar to *in vivo* perfection. In contrast, conventional buffer systems do not allow quantitative occupation of the ribosomal tRNA binding sites at Mg^{2+} concentration below 10 mM (Rheinberger and Nierhaus, 1987). Furthermore, Mg^{2+} concentrations above 20 mM block protein synthesis, therefore we chose to compare conventional buffers containing Mg^{2+} concentrations at these boundaries, namely 10 and 20 mM.

	A6/A10	A6/A20	A10/A20		A6/A10	A6/A20	A10/A20
1G	n.d.	n.d.	n.d.	**39U**	**0.29**	**0.31**	1.05
2C	n.d.	n.d.	n.d.	**40C**	**0.46**	*0.59*	1.27
3C	n.d.	n.d.	n.d.	**41C**	**0.38**	*0.55*	1.43
4C	n.d.	n.d.	n.d.	**42-43C**	**0.39**	*0.57*	1.49
5G	n.d.	n.d.	n.d.	**44G**	*0.78*	0.92	1.18
6G	n.d.	n.d.	n.d.	**45U**	1.07	0.96	0.90
7A	**0.43**	**0.39**	0.90	**46G**	1.01	1.18	1.17
8U	**0.31**	**0.34**	1.10	**47U**	0.88	0.80	0.90
9A	*0.76*	*0.75*	0.98	**48C**	1.16	1.28	1.10
10G	*0.70*	0.82	1.17	**49C**	*0.70*	0.91	1.30
11C	**0.44**	0.63	1.45	**50U**	**0.47**	**0.45**	0.96
12U	**0.41**	**0.37**	0.92	**51U**	*0.51*	*0.51*	1.00
13C	**0.45**	*0.54*	1.22	**52G**	*0.77*	1.13	1.47
14A	*0.54*	*0.54*	1.00	**53G**	*0.60*	*0.78*	1.30
15G	*0.61*	*0.72*	1.17	**54U**	*0.63*	*0.71*	1.13
16U	**0.38**	**0.36**	0.94	**55U**	0.85	0.84	0.99
17C	*0.58*	*0.63*	1.09	**56C**	1.12	1.31	1.17
18G	*0.63*	*0.70*	1.12	**57G**	*0.51*	*0.67*	1.31
19G	*0.65*	*0.75*	1.14	**58A**	*0.64*	*0.66*	1.04
20U	*0.61*	*0.57*	0.94	**59U**	*0.58*	*0.56*	0.96
21A	0.87	0.91	1.04	**60U**	*0.60*	*0.60*	1.02
22G	*0.64*	*0.72*	1.13	**61C**	1.04	1.13	1.09
23A	*0.63*	*0.57*	0.91	**62C**	0.88	0.95	1.09
24G	**0.36**	**0.49**	1.35	**63G**	*0.61*	*0.69*	1.13
25C	**0.29**	**0.35**	1.22	**64A**	*0.77*	*0.71*	0.93
26A	**0.46**	**0.43**	0.94	**65G**	**0.46**	*0.58*	1.25
27G	*0.55*	*0.67*	1.23	**66U**	**0.45**	**0.48**	1.06
28G	**0.36**	**0.42**	1.16	**67C**	n.d.	n.d.	n.d.
29G	**0.33**	**0.35**	1.06	**68C**	n.d.	n.d.	n.d.
30G	**0.27**	**0.27**	1.02	**69G**	n.d.	n.d.	n.d.
31A	**0.31**	**0.34**	1.08	**70G**	n.d.	n.d.	n.d.
32U	**0.34**	**0.39**	1.14	**71G**	n.d.	n.d.	n.d.
33U	**0.45**	*0.50*	1.12	**72C**	n.d.	n.d.	n.d.
34G	*0.70*	0.94	1.34	**73A**	n.d.	n.d.	n.d.
35A	*0.72*	0.82	1.14	**74C**	n.d.	n.d.	n.d.
36A	0.85	0.85	1.00	**75C**	n.d.	n.d.	n.d.
37A	*0.76*	*0.79*	1.03	**76A**	n.d.	n.d.	n.d.
38A	*0.67*	*0.68*	1.02				

Table 3.2.2.1: Accessibility pattern of thioated $tRNA^{Phe}$ under various buffer conditions. A6, accessibility under polyamine conditions (6 mM Mg^{2+}); A10 and A20, accessibility under conventional buffer conditions without polyamines at 10 and 20 mM Mg^{2+}, respectively; bold numbers, the intensity ratio of the corresponding bands is below 0.49 (e.g. A7, 0.43 for A6/A10 means that the accessibility of phosphate at position A7 is protected more under polyamine buffer conditions than under conventional buffer conditions); italicized numbers, the ratio is between 0.5 and 0.79; underlined numbers, the ratio is above 1.15; ratios between 0.8 and 1.14 are not considered to differ significantly . The numbers are averages of up to four experiments, the standard deviation was below 10%. n.d., not determined.

Little discernable difference was observed between the protection patterns under conventional buffer conditions at 10 or 20 mM Mg^{2+}, whereas the intensities at a number of positions generated under polyamine buffer differ from the corresponding ones at conventional conditions. For example, bases C40-C43 are weaker than the corresponding bands in the 10 and 20 mM Mg^{2+} lanes. Quantitative analyses of four such experiments was averaged, and the results

are presented in Table 3.2.2.1 and they were presented in Figure 3.2.2.2 in a color code.

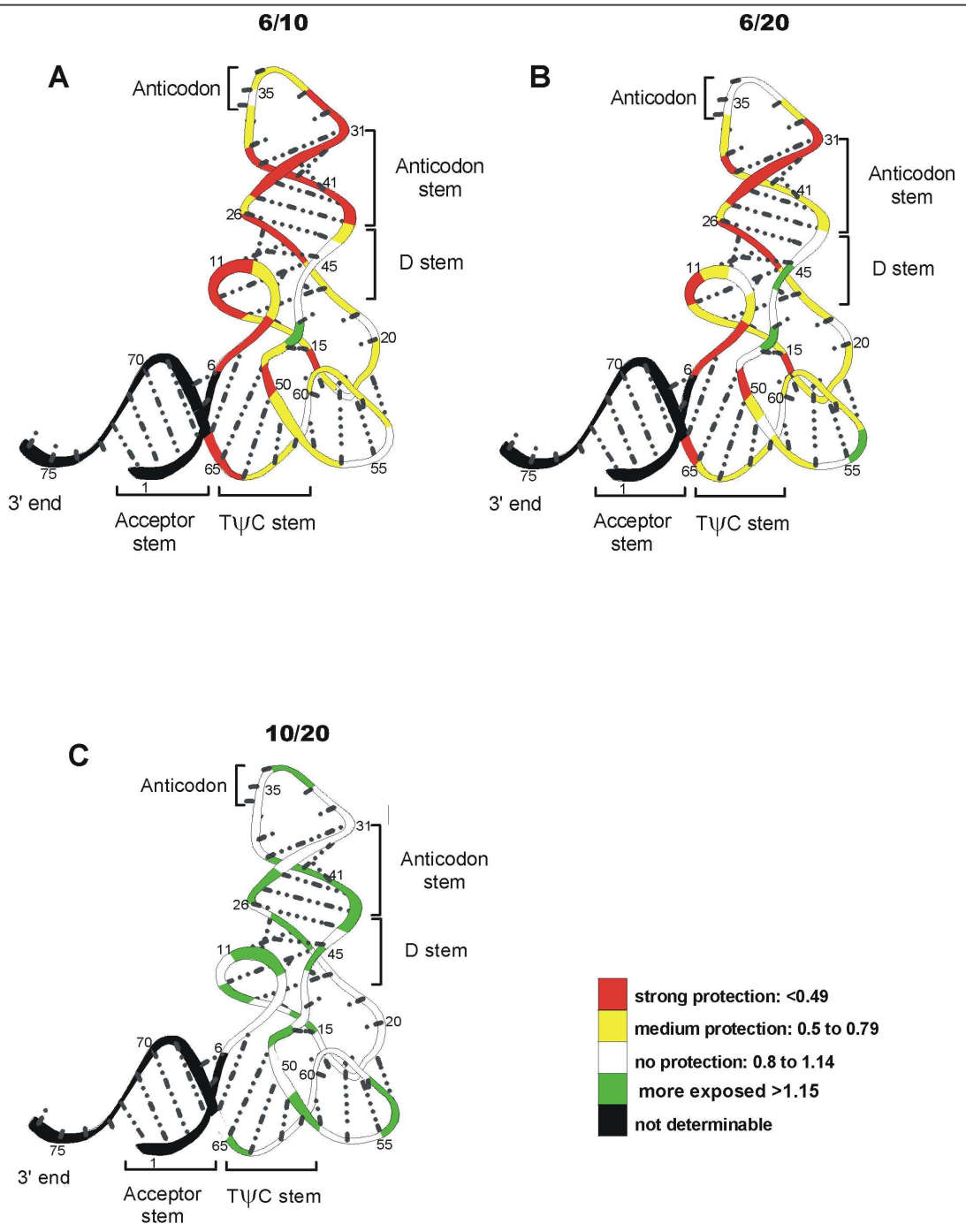

Figure 3.2.2.2: Color code representation of the Table 3.2.2.1. 6, accessibility under polyamine conditions (6 mM Mg^{2+}); 10 and 20, accessibility under conventional buffer conditions without polyamines at 10 and 20 mM Mg^{2+}, respectively.

Generally, phosphates located in the tRNA loops were equally accessible to iodine-induced cleavage under all buffer conditions tested, e.g. bases of the anticodon loop G34-A38 and those of the D loop A14-A21, whereas phosphates located in many helical regions were less accessible under polyamine conditions, e.g. phosphates of the anticodon stem G28-A31 and U39-C43. The accessibility of a few bases was magnesium concentration-dependent, e.g. C49 and G53 were more accessible under conditions of 10 mM Mg^{2+} than 20 mM.

P_i State

Figure 3.2.2.3 shows a representative footprinting gel for a deacylated $tRNA^{Phe}$ in P_i state under different buffer conditions. A pattern specifically resulting from protections by the ribosome matrix was assessed by normalization against the "background" protection that results in the absence of ribosome, i.e. in the corresponding buffer solution only. Thus the difference pattern generated represents specifically the protections of a tRNA by the ribosome. The results were shown in color code in Figure 3.2.2.4. Surprisingly, the difference patterns were remarkably similar to one another regardless of the buffer conditions used. The difference pattern showed strong global protection of the bound tRNA similar to previous observations (Dabrowski et al., 1995).

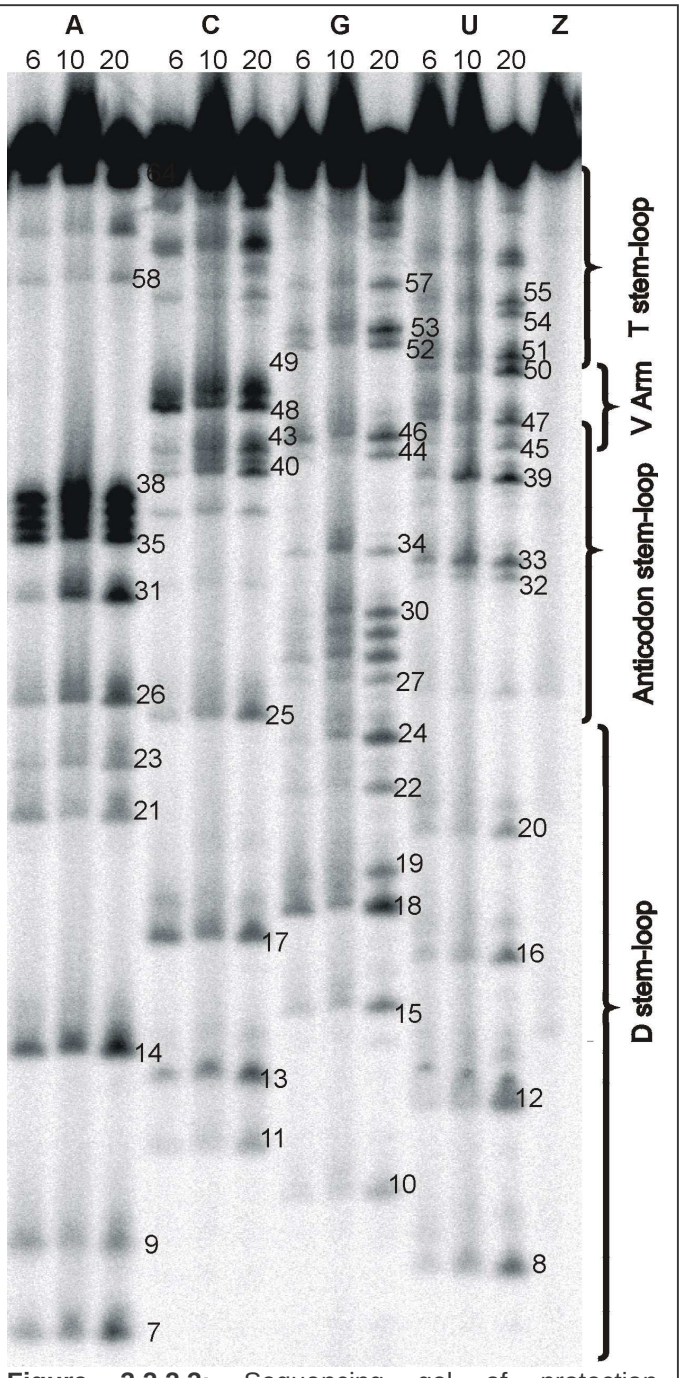

Figure 3.2.2.3: Sequencing gel of protection experiments with thioated $tRNA^{Phe}$ in Pi state. $tRNA^{Phe}$ was either in a buffer containing 6 mM Mg^{2+} and polyamines or in conventional buffers with 10 and 20 mM Mg^{2+} without polyamines (lanes marked with 6, 10 and 20, respectively). The numbers next to the bands indicate the nucleotide positions, structural elements of the tRNA are indicated on the right-hand side.

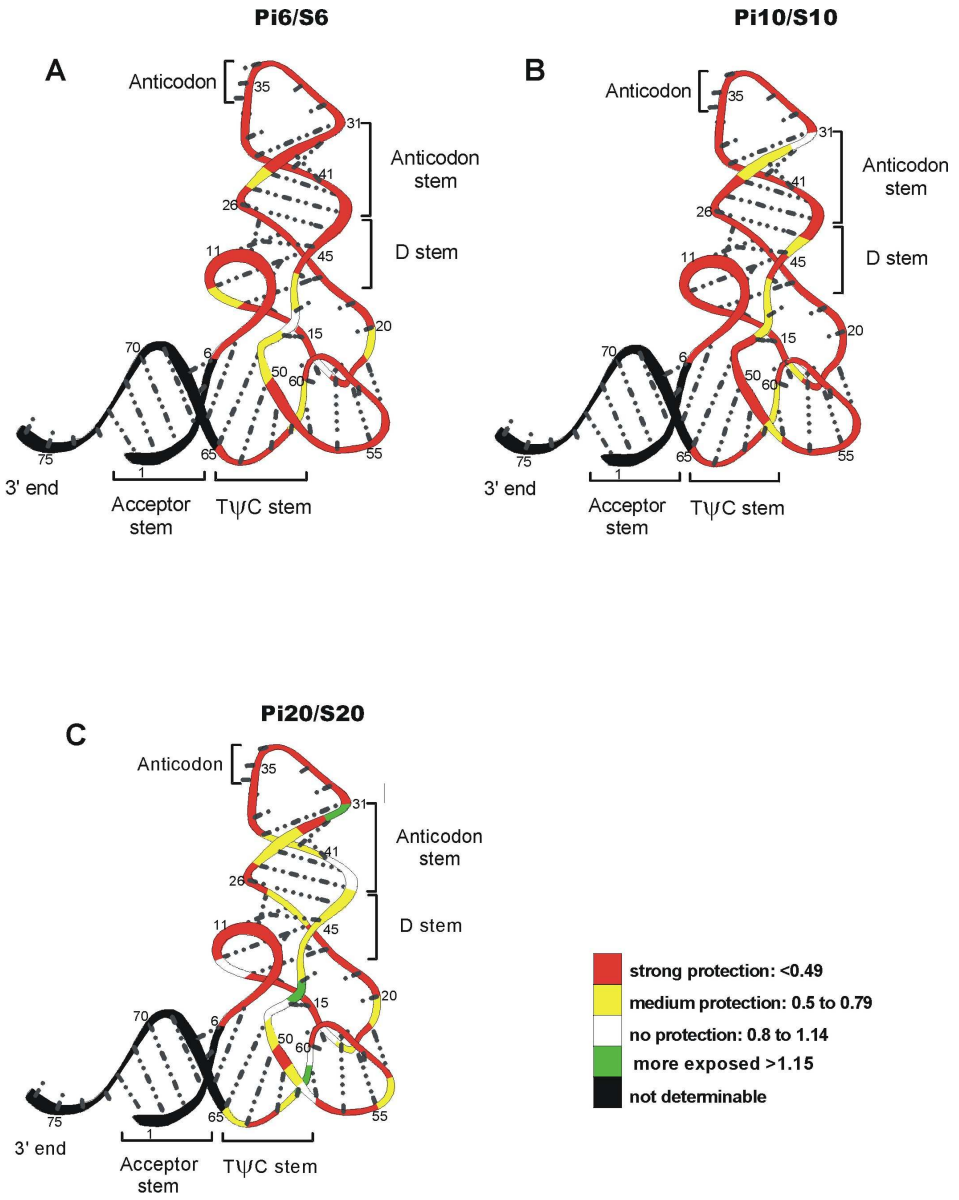

Figure 3.2.2.4: Color code representation of the iodine cleavage experiments in Pi complexes. 6, accessibility under polyamine conditions (6 mM Mg^{2+}); 10 and 20, accessibility under conventional buffer conditions without polyamines at 10 and 20 mM Mg^{2+}, respectively. Pi means tRNA in the P site of 70S and S means the cleavage of tRNAs on the solution.

However there were a few exceptions; A31, C49, C61, and C62 showed less protection under conventional buffer conditions than polyamine, and one strand of the anticodon stem, U39-G46, was specifically less protected under 20 mM Mg^{2+} buffer conditions.

3.2.3 Addition of mRNA Results in Additional Protection of the Anticodon Stem-Loop of a P Site-Bound tRNA

It is known that tRNA can bind to the 70S ribosome in the absence of the cognate mRNA. In order to determine the specificity of the protection pattern of the P site bound $tRNA^{Phe}$ and also to understand the effect of mRNA overall, the protection pattern of $tRNA^{Phe}$ was analyzed in the presence and absence of mRNA. Comparison of the protection pattern of the $tRNA^{Phe}$ was

	A	C	G	U	Z
No mRNA	0,26	0,34	0,34	0,30	0,31
PolyU	0,54	0,70	0,75	0,55	0,76
PolyA	0,24	0,28	0,37	0,25	0,24

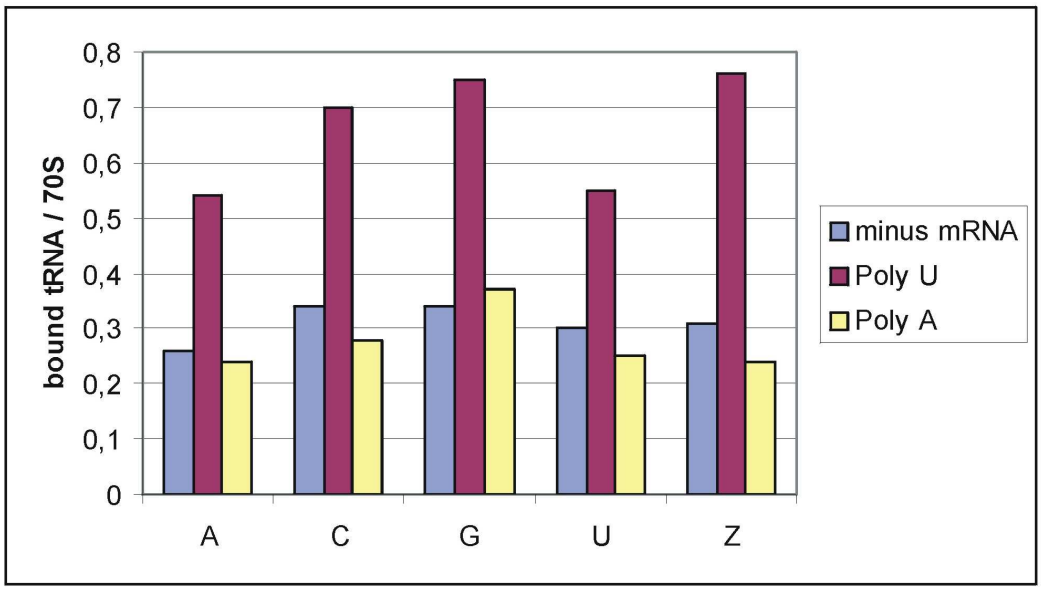

Figure 3.2.3.1: Binding of transcribed thioated tRNAs (A, C, G, U) in the presence or absence of mRNAs. Z is the control with non-thioated transcribed $tRNA^{Phe}$.

done in the presence of cognate poly(U) and non-cognate poly(A) mRNA and in the absence of mRNA (Figure 3.2.3.1). Under the conditions applied approximately 30% of non-programmed ribosomes bound a tRNA, and this value was two-fold increased by adding cognate poly(U). Interestingly, in the presence of non-cognate mRNA (poly(A)) the same binding efficiency was found as in the absence of mRNA. The constantly observed slightly decreased binding efficiency in the presence of poly(A) might be explained by

a possible interference of codon and non-cognate anticodon at the codon region of the P site counteracting the tRNA binding. Binding of the transcribed control tRNA which does not contain any thioated nucleotide showed the same behavior as thioated tRNAs proving that the introduction of a sulfur atom in the phosphate backbone of the phosphorothioated tRNAs has no negative effect in functional assays.

The complexes were prepared as following: The re-associated 70S ribosomes in a concentration of 60-100 pmol were incubated in a volume of 125 µl with either 6-8 molar excess of the poly(U) fraction number 21 (see section 3.1.2) or 60 µg of poly(A). For minus mRNA experiments no mRNA were added. Deacyl-$tRNA^{Phe}$ in a 0.8-fold molar ratio to ribosomes was bound to the P site. Binding conditions were $H_{20}M_6N_{150}SH_4Sd_2Sp_{0.05}$. After iodine cleavage (with a 1 mM final volume of iodine), complexes purified via spun column (see section 2.5.5.3) and ribosomal proteins were removed by phenol extraction. tRNA fragments were precipitated by EtOH precipitation and an amount of 10,000 dpm was loaded per lane. Figure 3.2.3.2 is one of the representative gels of these experiments. This experiment was repeated three times and the results were presented graphically, where the x-axis represents the positions of the phosphate residues of $tRNA^{Phe}$ (theoretically 1-76), and the y-axis the relative accessibility of each position (Figure 3.2.3.3). Upon addition of mRNA, there is a conspicuous change in protection extending between positions 29 and 39. This region of protection corresponds with the anticodon stem-loop and three additional bases of the 3'-strand of the anticodon stem. Positions prior to 28 and those subsequent to position 40 exhibit protection patterns that remain unaltered in the presence or absence of poly(U). Exceptions include bases A26, C48, and C61/62 (the latter could not be separated in the sequencing gel). Our results are in good agreement with similar experiments performed with $tRNA_m^{Met}$ in the presence and absence of the heteropolymeric MF-mRNA, an mRNA which contains a unique AUG codon [Sebastian Patzke, Diploma thesis FU Berlin, 1998]. Furthermore, protection of $tRNA^{Phe}$ was assessed in the presence of the non-cognate poly(A) mRNA, which exhibited a pattern similar to that obtained in the absence of mRNA (see Figure 3.2.3.3) thus

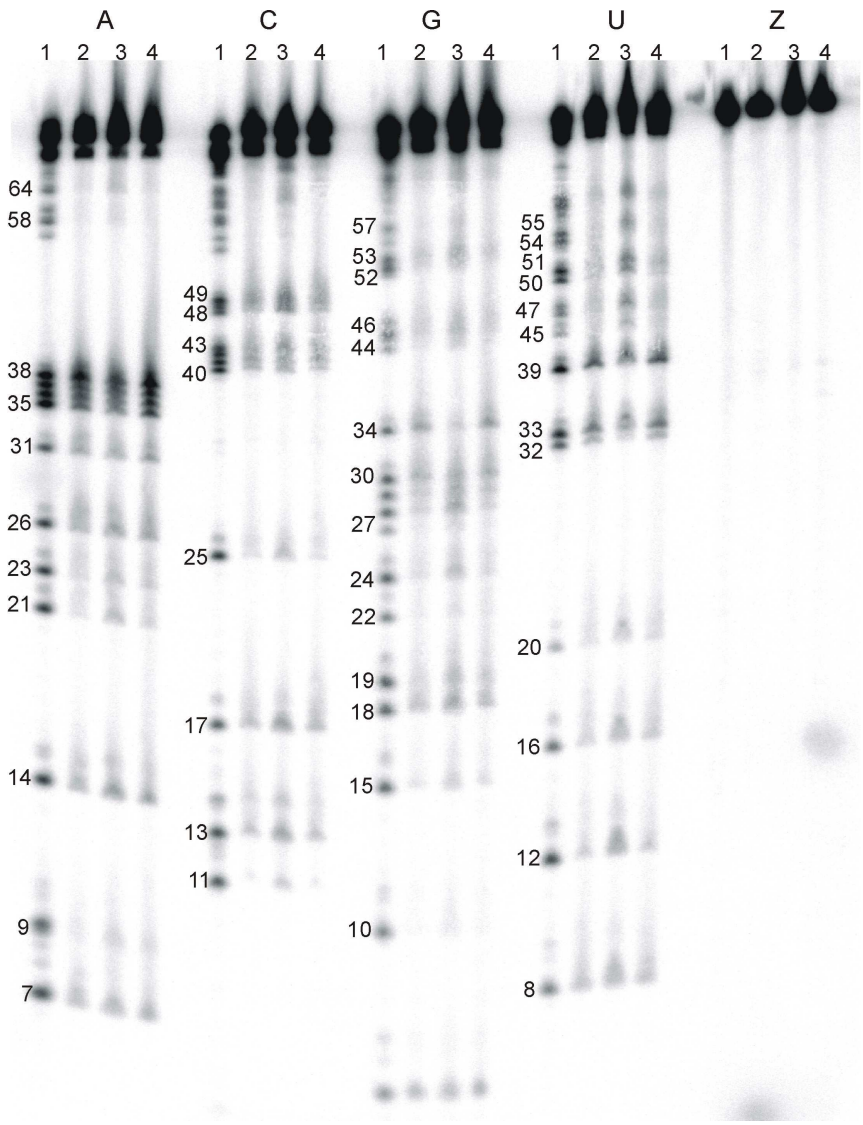

Figure 3.2.3.2: Sequencing gel of protection experiments with thioated $tRNA^{Phe}$. $tRNA^{Phe}$ was either in solution, or bound to the P site of the 70S ribosome in the presence of no mRNA or poly(U) or poly(A) (lanes marked with 1 to 4, respectively). The numbers next to the bands indicate the nucleotide positions. A, C, G, U show the thioated nucleotides in the tRNA and Z is the control transcribed RNA without phosphorothioation.

showing that tight contacts of the tRNA with the 30S subunit within the 70S ribosome depend on codon-anticodon interaction at the P site.

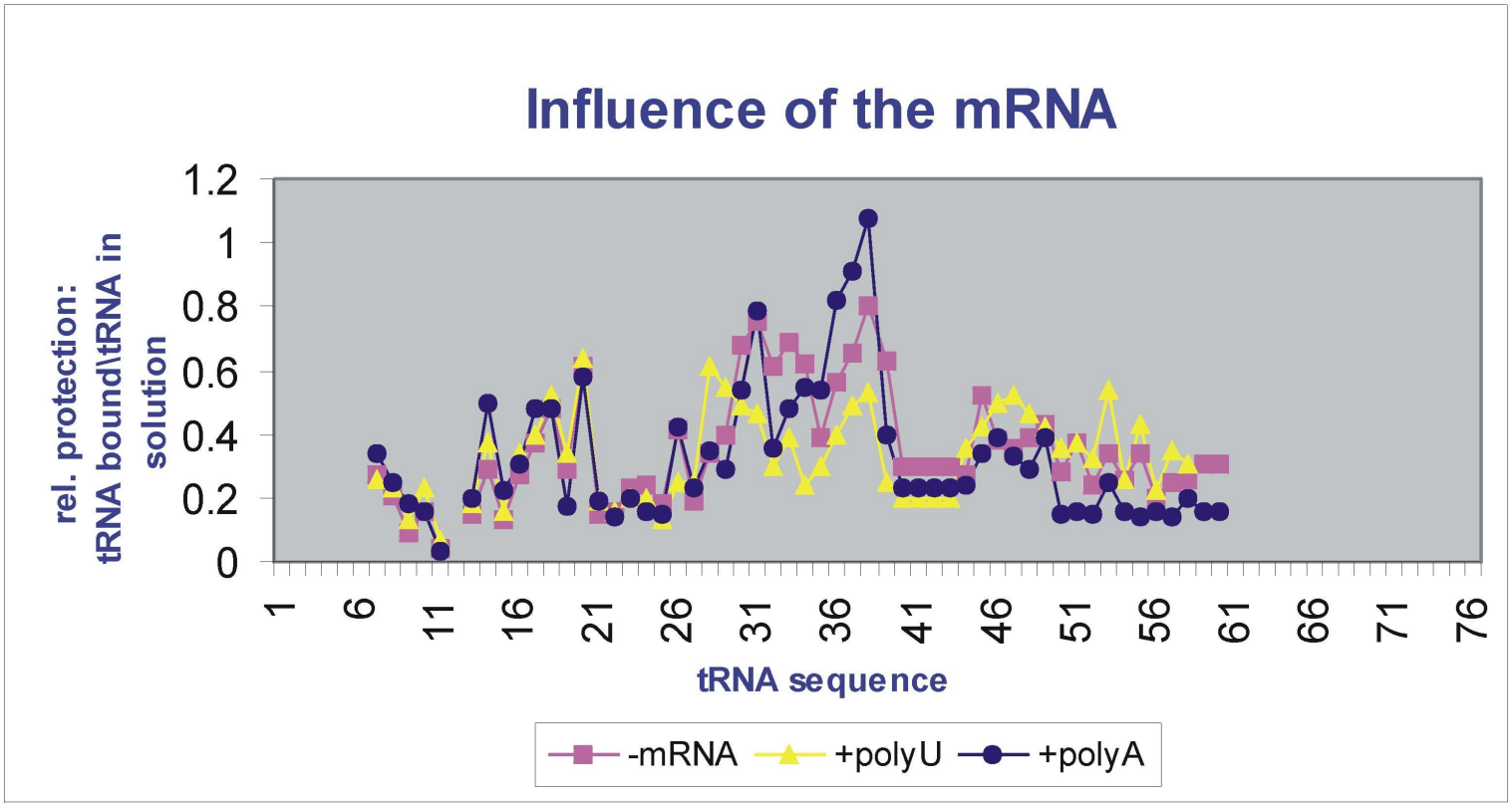

Figure 3.2.3.3: Graphical presentation of the protection patterns of $tRNA^{Phe}$ in the Pi state in the presence or absence of mRNA.

3.2.4 Oscillating Ribosomes

3.2.4.1 Puromycin Reaction with Ac[^{14}C]Phe-[^{32}P]tRNA^{Phe}

The antibiotic puromycin mimics the CCA end of the Tyr-tRNA^{Tyr}, binds to the A site of the ribosome and is partner of a P-site bound acyl-tRNA in forming a peptide-bond. The result is that the AcPhe-tRNA at the P site is converted to a deacylated tRNA at this site. Does the tRNA pattern at the P site change upon peptide-bond formation?

A general scheme of the experiments is shown in Figure 3.2.4.1.1. The experimental procedure was as following: 100 pmol re-associated 70S ribosomes were incubated in a volume of 150-175 µl with a 6-8 molar excess of the MFV-mRNA. 30-40 pmol Ac[^{14}C]Phe-[^{32}P]tRNA^{Phe} was bound to the P site of the MFV-mRNA programmed 70S ribosome. Incubation reaction was done in 37 ℃ for 15 minutes under the buffer conditions of $H_{20}M_6N_{150}SH_4Sd_2Sp_{0.05}$. Unbound tRNA was removed by pelleting the complex (150-175 µl reaction mixture) through a 10% sucrose cushion (1-1.5 ml; 18 hours, 43,000 rpm, Beckman TLA 100.3 rotor). Pellets were dissolved in 100 µl binding buffer and recovery was calculated with the spectrophotometric measurement of the ribosome. Generally the yield was between 60-80%. The bound Ac[^{14}C]Phe-[^{32}P]tRNA^{Phe} was determined in two ways: Either a direct measurement via direct counting the radioactivity in a volume unit or by measuring the radioactivity of volume unit that could be collected on a nitrocellulose filter. According to the direct counting binding of the phosphorothioated Ac[^{14}C]Phe-[^{32}P]tRNA^{Phe}s was found between 0.4 to 0.65 tRNA per ribosome. Filter assay results were in good agreement with the direct measurement, and slightly decreased values in the filter assays are due to the harsh filtration condition, where some of the tRNAs might be washed off the ribosome. The puromycin reaction did not change during the pelleting procedure changed thus proving that the tRNAs did not change their functional position on the ribosome.

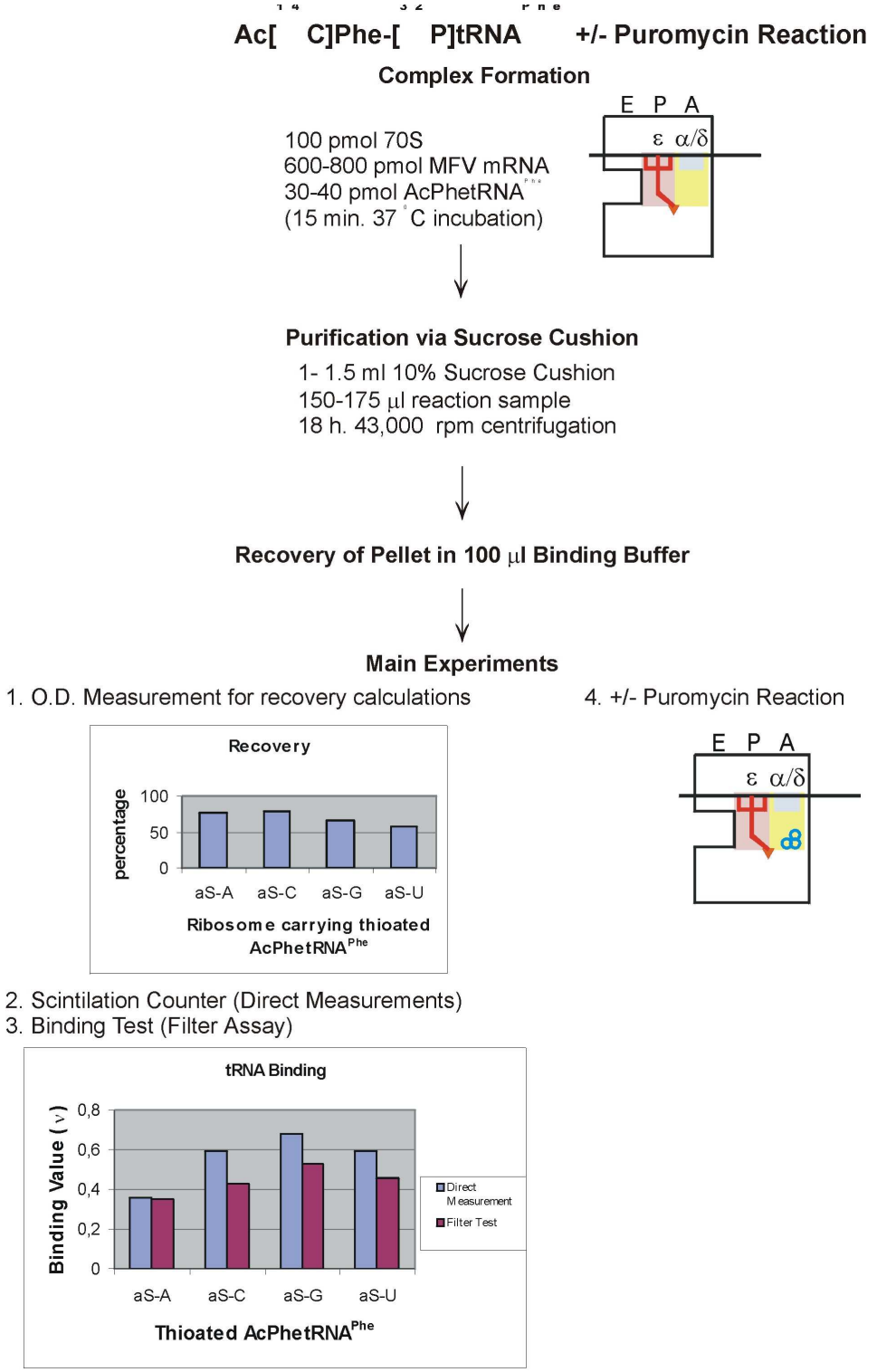

Figure 3.2.4.1.1: General scheme of the experiment, where the effect of puromycin reaction was checked in the protection pattern of P site bound Ac[^{14}C]Phe-[^{32}P]tRNA^{Phe}.

Iodine cleavage was the next step after sucrose cushion treatment to analyze the protection pattern of the P site bound Ac[^{14}C]Phe-[^{32}P]tRNA^{Phe} and was performed as in the method section (section 2.5.5.2). One of the representative gels of the cleavage experiments is shown in the Figure 3.2.4.1.2.

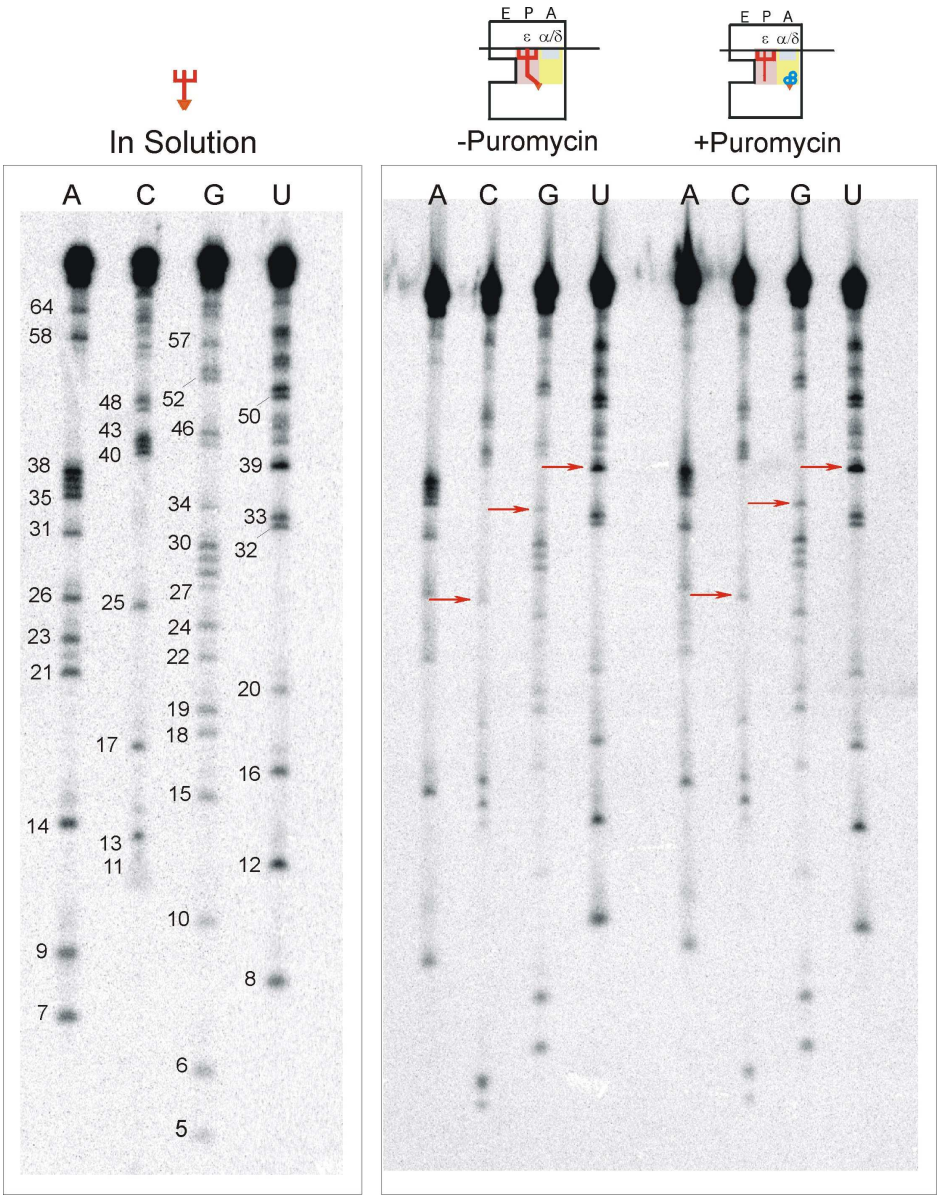

Figure 3.2.4.1.2: 13% Acrylamide sequencing gel of protection experiments with thioated Ac[^{14}C]Phe-[^{32}P]tRNA^{Phe}. Left panel, Ac[^{14}C]Phe-[^{32}P]tRNA^{Phe} cleavage in solution. The right panel shows the cleavage pattern of the P site bound Ac[^{14}C]Phe-[^{32}P]tRNA^{Phe} in the absence or presence of the puromycin. The numbers next to the bands indicate the nucleotide positions. A, C, G, U are the tRNAs with the corresponding phosphorothioated nucleotide incorporation. ↓, Ac[^{14}C]Phe-[^{32}P]tRNA^{Phe}. The red arrows show some of the cleavage differences due to protection

A pattern specifically resulting from protections by the ribosome matrix was calculated by normalization against the accessibility of the corresponding phosphate residues of a tRNA in solution. Thus the difference pattern generated represents specifically the protections of a tRNA by the ribosome. The results were shown in color code in Figure 3.2.4.1.3. Figure 3.2.4.1.4 is the graphic representation of the color code, where the x-axis indicates the positions of the phosphates of the tRNA and y-axis the relative accessibility.

According to our results, although overall protection pattern of the Ac[^{14}C]Phe-[^{32}P]tRNA^{Phe} is not changing with the puromycin reaction, some regions of the P site bound tRNA are more protected in the absence of puromycin, especially the anticodon and D stem loop regions. Some of the examples are the positions13, 25, 32,34 and 39. Nucleotide 34 is an example that might be incorrectly assigned in the color code. The reason is that a relative protection is a value in the range of 0.7 to 1.3. This residue is just above this border (0.72) as AcPhe-tRNA (minus puromycin) and just below (1.3) as deacylated tRNA (plus puromycin).

	A	B			A	B
1G				39U	0,59	1,1
2C				40C	0,27	0,39
3C				41C	0,27	0,39
4C				42C	0,27	0,39
5G				43C	0,27	0,39
6G	0,90	0,82		44G	0,63	0,53
7A	0,40	0,37		45U	0,66	0,68
8U	0,86	0,8		46G	0,57	0,64
9A	0,10	0,21		47U	0,88	0,94
10G	0,16	0,37		48C	0,63	0,84
11C	1,13	0,83		49C	0,66	0,67
12U	0,60	0,77		50U	0,64	0,67
13C	0,57	0,9		51U	0,87	0,94
14A	0,44	0,34		52G	0,58	0,67
15G	0,29	0,44		53G	1,51	1,53
16U	0,48	0,56		54U	0,57	0,54
17C	0,36	0,46		55U	0,74	0,53
18G	0,40	0,66		56C		
19G	0,36	0,32		57G	0,55	0,47
20U	0,64	0,87		58A	0,26	0,16
21A	0,24	0,23		59U	0,77	0,79
22G	0,23	0,31		60U	0,77	0,79
23A	0,25	0,22		61C	1,07	0,82
24G	0,36	0,54		62C	1,07	0,82
25C	0,24	0,49		63G		
26A	0,37	0,3		64A	0,64	0,48
27G	0,32	0,44		65G		
28G	0,43	0,58		66U		
29G	0,55	0,66		67C		
30G	0,72	0,98		68C		
31A	0,64	0,77		69G		
32U	0,36	0,75		70G		
33U	0,83	0,87		71G		
34G	0,72	1,3		72C		
35A	1,08	0,92		73A		
36A	1,08	0,92		74C		
37A	1,08	0,92		75C		
38A	1,08	0,92		76A		

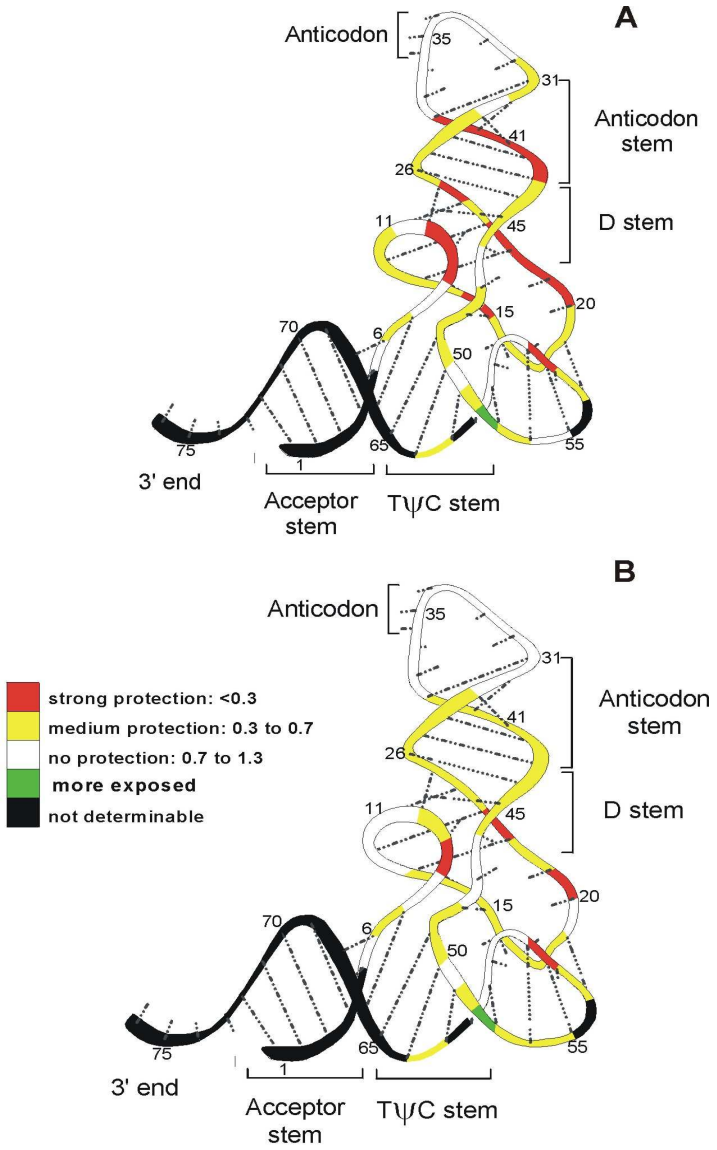

Figure 3.2.4.1.3: The accessibility data are shown on the left side. The numbers are averages of two experiments. On the right side the color code presentation of the accessibility patterns of the P site bound Ac[^{14}C]Phe-[^{32}P]tRNA^{Phe} in the absence (A) and in the presence (B) of puromycin are shown. Bands are enboxed that could not been separated and thus were calculated together.

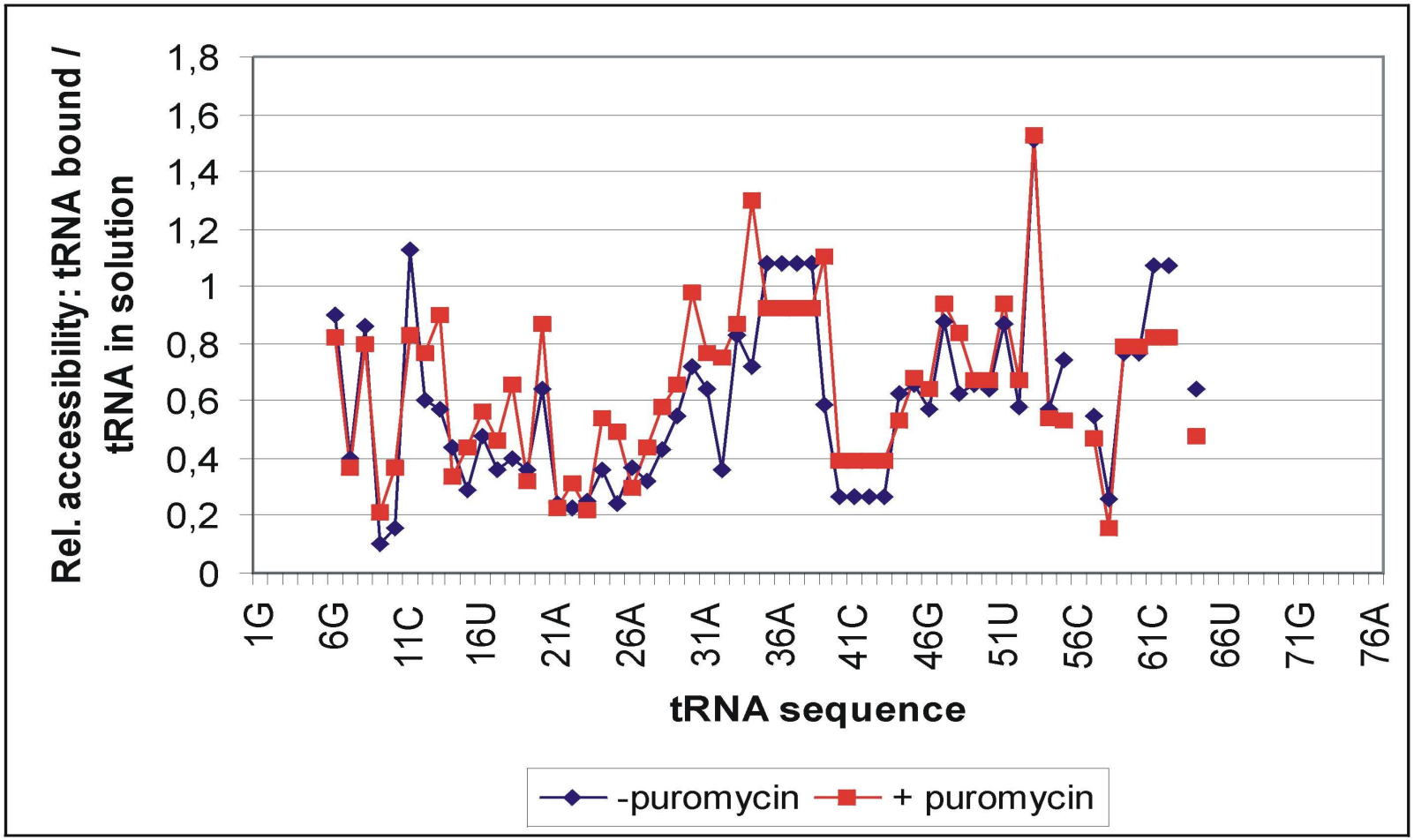

Figure 3.2.4.1.4: Graphic presentation of the protection experiments of the Ac[^{14}C]Phe-[^{32}P]tRNA^{Phe} in the Pi state in +/- puromycin reaction.

3.2.4.2 Dipeptide bond formation

The experiment in this section should analyze a complete elongation cycle. We wanted to follow the change of a protection pattern of a tRNA on the ribosome, when it is moving from one tRNA binding site to the adjacent one. For this experiment, an mRNA with three codons (MFV) was used. The experiment starts with a PRE complex containing a $tRNA_f^{Met}$ in the P site and thioated Ac[^{14}C]Phe-[^{32}P]$tRNA^{Phe}$ in the A site, thus checking the A site bound tRNA protection pattern which mimics a tRNA right after the peptide bond formation but before translocation. With the translocation reaction, the same tRNA moves to the P site in the POST complex. According to the α–ε model the tRNA should not change the protection pattern, since tRNAs are carried by a movable domain. The results of these two complexes led to the α-ε model (Dabrowski et al., 1998). Here, additionally we wanted to go one step further by binding the next aminoacyl-tRNA, namely [^{3}H]Val-$tRNA^{Val}$ as a ternary complex to the A site. Upon peptide-bond formation AcPhe-Val-$tRNA^{Val}$ will be at the A site and the thioated deacyl-tRNA remains at the P site. Does the deacylated tRNA changes its protection pattern as compared to the AcPhe-Val-tRNA at the P site?

Complex formation was done in the following way: 150 pmol re-associated 70S ribosomes were incubated in a volume of 375 µl with 8 molar excess of the MFV-mRNA (1200 pmol). 375 pmol of $tRNA_f^{Met}$, which is in 2.5 molar excess to the 70S ribosome, was bound to the P site. 40-60 pmol thioated Ac[^{14}C]Phe-[^{32}P]$tRNA^{Phe}$ was then bound to the A site of the MFV-mRNA programmed 70S ribosome under the $H_{20}M_6N_{150}SH_4Sd_2Sp_{0.05}$ conditions. 50 µl out of 375 µl reaction was taken for both the binding test (approximately 0.6 tRNA was bound per 70S ribosome) and the puromycin reaction. Unbound tRNA was removed from the complex by pelleting the complex through a sucrose cushion as described above. Pellets were dissolved in 320 µl binding buffer and the recoveries were around 50-60%. The binding of the Ac[^{14}C]Phe-[^{32}P]$tRNA^{Phe}$ did not change during the pelleting step. 40 µl of this reaction was used for the iodine cleavage, while the rest was frozen to continue later the preparation for the POST complexes. One minute iodine

exposure (1 mM final concentration) was stopped with DTT (2 mM final concentration). After phenol extraction and EtOH precipitation, tRNA pellets were dissolved in H_2O and loading buffer and samples were kept at –20 ℃ until the rest of the experiments was finished and all samples (Pre I, Post, Pre II) could be loaded onto the same gel (Figure 3.2.4.2.1).

Post complex were prepared by addition of EF-G to the reaction mixture. Again the same procedure was executed as explained above until the end of iodine cleavage.

For the PRE-II complex, [^{3}H]Val-tRNA^{Val} was added to the complex as a pre-prepared ternary complex. The ternary complex (aminoacyl-tRNA•EF-Tu•GTP) was formed immediately before its addition to the binding assay: aminoacyl-tRNA (2 pmol per pmol of 70S ribosomes), 0.5 mM GTP, and EF-Tu (2 pmol per pmol of aminoacly-tRNA) were preincubated for 2 min at 37 ℃ under the ionic conditions of the binding buffer and were added to the reaction mixture. In this step we did not remove the unbound Val-tRNA by a pelleting step through a sucrose cushion, since we were just analyzing the resulting thioated [^{32}P]tRNA^{Phe} at the P site. In other words, the sample was directly subjected to an iodine cleavage step.

The radioactivity of all samples were measured in the scintillation counter and 2000 dpm/lane per sample was loaded onto the 13% gel (Figure 3.2.4.2.1). The data were analyzed employing the Image-Quant program and the results are presented in Table 3.2.4.2.1. A graphic representation of the calculations is shown in the Figure 3.2.4.2.2.

Generally, the protections of the nucleotides of the AcPhe-tRNA can be assigned to one out of three groups. The first one comprises residues, where they show the same pattern in the PRE-I and POST complexes but deviate in the PRE-II complex. For example, nucleotides between 6-12 show the same protection pattern in PRE-I and POST complexes. Also some parts of the anticodon stem-loop area (e.g. nucleotides 40-44) and to the T stem-loop region (e.g. nucleotides 54-62) can be given as examples to this group. The

second group shows the same pattern in the POST and PRE-II complexes, e.g. nucleotides 13, 16 and 45. The last one is characterized by the same pattern in the PRE-I and PRE-II complexes, note the very distinct similarities for the PRE-I and PRE-II complexes in the nucleotides 52 and 53.

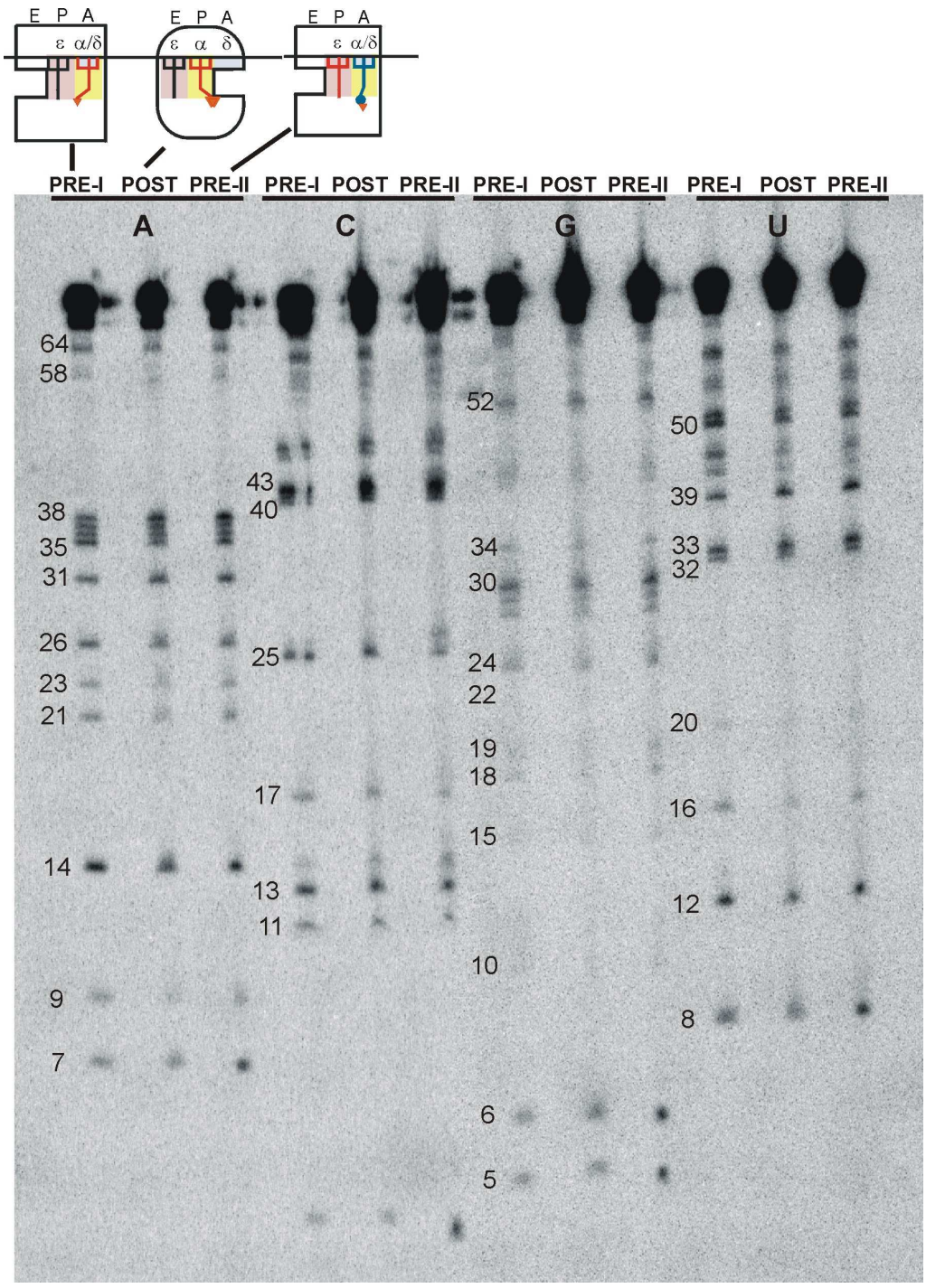

Figure 3.2.4.2.1: 13% AA sequencing gel of protection experiments for the oscillating ribosome. Complex Pre-I is the one with $tRNA_f^{Met}$ in the P site and thioated Ac[^{14}C]Phe-[^{32}P]$tRNA^{Phe}$ in the A site of the ribosome. Post complex is after translocation and Pre-II complex was prepared with the binding of Val-[^{3}H]$tRNA^{Val}$ to the A site after translocation. The numbers next to the bands indicate the nucleotide positions. A, C, G, U are the tRNAs with the corresponding phosphorothioated nucleotide incorporation. ⍊, $tRNA_f^{Met}$; ⍊, Ac[^{14}C]Phe-[^{32}P]$tRNA^{Phe}$; ⍊, Val-[^{3}H]$tRNA^{Val}$

	Pre-I /Sol	Post/Sol	Pre-II/Sol			Pre-I/Sol	Post/Sol	Pre-II/Sol
1G					39U	0,29	0,38	0,41
2C					40C	0,82	0,77	0,65
3C					41C	0,82	0,77	0,65
4C					42C	0,82	0,77	0,65
5G					43C	0,82	0,77	0,65
6G	0,75	0,64	1,56		44G	0,53	0,42	0,69
7A	0,39	0,32	0,88		45U	0,72	0,47	0,39
8U	0,53	0,49	0,87		46G	0,4	0,21	0,45
9A	0,32	0,19	0,26		47U	0,9	0,46	0,60
10G	0,26	0,27	0,33		48C	0,87	1,01	1,06
11C	2	1,57	1,16		49C	0,9	0,69	0,73
12U	0,59	0,34	0,41		50U	0,84	0,59	0,66
13C	1,35	0,88	0,76		51U	0,52	0,38	0,38
14A	1,16	0,63	0,82		52G	1,48	1,08	1,39
15G	0,04	0,05	0,30		53G	1,48	1,08	1,39
16U	0,3	0,14	0,21		54U	0,42	0,31	0,45
17C	0,6	0,39	0,33		55U	0,43	0,44	0,47
18G	0,1	0,18	0,55		56C	0,62	0,59	0,53
19G	0,18	0,16	0,29		57G	0,43	0,34	0,48
20U	0,3	0,19	0,33		58A	0,16	0,20	0,27
21A	0,44	0,19	0,34		59U	0,59	0,40	0,44
22G	0,25	0,13	0,15		60U	0,59	0,40	0,44
23A	0,36	0,16	0,32		61C	0,98	0,72	0,62
24G	0,44	0,32	0,45		62C	0,98	0,72	0,62
25C	0,7	0,92	0,62		63G			
26A	0,7	0,52	0,57		64A	0,78	0,64	0,73
27G	1,04	0,49	0,71		65G			
28G	0,6	0,38	0,57		66U			
29G	1,21	0,82	1,46		67C			
30G	1,21	0,82	1,46		68C			
31A	0,81	0,99	1,10		69G			
32U	0,31	0,40	0,38		70G			
33U	0,65	0,60	0,76		71G			
34G	0,68	0,44	0,76		72C			
35A	0,72	0,44	0,62		73A			
36A	0,56	0,50	0,56		74C			
37A	0,45	0,46	0,50		75C			
38A	0,33	0,45	0,57		76A			

Table 3.2.4.2.1: Protection patterns of the thioated tRNA moiety of Ac[^{14}C]Phe-[^{32}P]tRNA^{Phe} in three different complexes, namely Pre-I, Post, Pre-II. Red color stands for strong protection, yellow for the medium and grey for no protection. Exposed positions were shown in green. Bands are enboxee that coud not be separated and thus were calculated together.

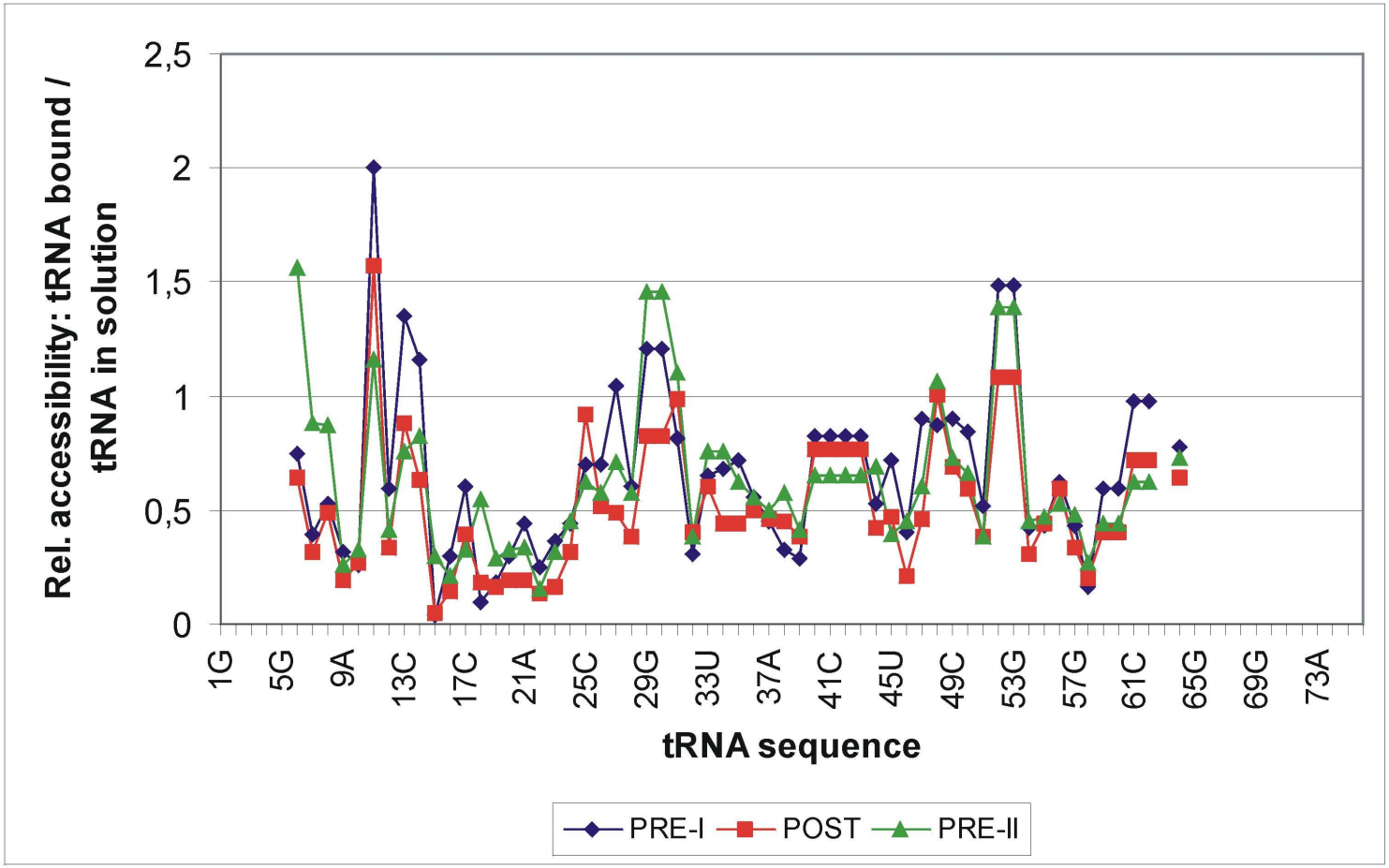

Figure 3.2.4.2.2: Graphic representation of the protection experiments in the oscillating ribosome. The x-axis shows the phosphate positions and the y-axis the relative accessibilities.

3.3 Computational Analysis

In this part of the work, we analyzed some of the footprinting experiments reported in a previous Ph.D. thesis of the group in more detail by comparing with the recent 5.5 Å X-ray map of the 70S complex. Analysis was performed in two steps. First, conservation of the neighboring ribosomal components and conservation of the tRNA bases adjacent to a number of strongly protected common phosphates between two different elongator tRNAs were analyzed. Second, the possible agreement between 5.5 Å map and the footprinting data for the contribution of each subunit to the overall distribution of contacts made with the P site tRNA was analysed. During these analyses Ras-Mol and Pov-Ray programs were used. The script files of the 5.5 Å X-ray map of the 70S complex was first analyzed in the Ras-Mol program (e.g. analysis of 10 Å neighborhood) and then transferred from Ras-Mol to the Pov-Ray. Figures 3.3.1.1. and 3.3.2.1 were mainly made with the Pov-Ray program.

3.3.1 Similar protection patterns are derived using distinct tRNA species

In order to test whether the protection pattern at the P site with deacylated $tRNA^{Phe}$ is specific for $tRNA^{Phe}$ species or whether it is representative for all tRNA species, protection experiments with a different elongator tRNA were previously performed (Schäfer, 1997; Schäfer et al., 2002). The tRNA chosen was elongator $tRNA_m^{Met}$ as it differs in sequence from $tRNA^{Phe}$ at 28 out of 76 comparable positions (37%). The protection pattern of $tRNA_m^{Met}$ is in general agreement with that of $tRNA^{Phe}$, although it displays overall weaker protection. In both tRNAs, parts of the TΨC and D-stem and the anticodon loops are strongly protected. Although the regions with strong protection comprise both paired and unpaired bases, they are predominantly found within exposed regions of the tertiary structure of the tRNA. Ten strong protections that are common between two different species of elongator tRNA, *viz.* $tRNA^{Phe}$ and $tRNA^{Met}$ were determined (Table 3.3.1.1).

Protected phosphate	upstream nucleoside (towards 5'-end)		downstream nucleoside (towards 3'-end)	
11		G10	+	Y11
30		G29		G30
32		A31	+	Y32
34	+	U33		G34
41		C40		C41
54	+	G53	+	T54
56	+	Ψ55	+	C56
58	+	R57	+	A58
59	+	A58		U59
60		U59	+	Y60

Table 3.3.1.1: Strongly protected bases in both $tRNA^{Phe}$ and $tRNA^{Met}$. +, universally conserved base; R, purine; Y, pyrimidine (universally semiconserved) (Schäfer et al., 2002).

Eight out of ten strong protections are adjacent to conserved bases of the tRNA (Table 3.3.1.1). A detailed inspection of the 5.5 Å map of the 70S complex revealed that the ribosomal components neighboring the ten strongly protected tRNA bases are also remarkably conserved (Table 3.3.1.2 and Figure 3.3.1.1). First we identified the 10 Å surroundings of these highly conserved ten tRNA bases using the 70S map. As a second step, we checked the conservation of the rRNAs and ribosomal proteins that we found in the area of 10 Å. The conservation data concerning rRNA were obtained from the Gutell Lab Pages (www.rna.icmb.utexas.edu/csi) and the sequences of ribosomal proteins are from the Sequence Retrieval System (www.expasy.ch/srs5/) and alignment followed (Corpet, 1988) according to prodes.toulouse.inra.fr/multalin/multalin.html.

The analysis reveals interesting results. Table 3.3.1.2 shows the summary of our analysis. Most of the rRNA bases that we found in the 10 Å area have >95% conservation in bacteria. Bases 1910, 1923, 1924, 2280, 2327 from 23S rRNA and 1230, 1341, 1339 from 16S rRNA are examples with this high degree of conservation (80-100% across all three phylogenetic domains).

5'-phosphate of tRNA base	Residue of rRNA or r-protein nearer than 10Å [rRNA/nt or r-prot/aa]	Evolutionary conservation eubact	3 domains
Y11	23S/1909, 1910 1923, 1924	80-90, ≥95 ≥95, ≥95	<80, 90-95 ≥95, <80
G30	16S/1230	≥95	80-90
	S13/Lys121	Lys or Arg at position 120	
Y32	16S/1341 S9/Ser126, Lys127, Arg128	≥95 126 and 127: ~50% cons. 128: ~90% conserved	≥95
G34	(anticodon: 16S/1400)		
C41	16S/1339, 1340	≥95, <80	≥95, <80
T54	23S/2280, 2327	≥95, ≥95	80-90, <80
C56	L5/Arg56 and Glu65	Arg or Lys at position 56 Arg or Lys at position *64*	
A58 U59 Y60	protected *via* tertiary folding of tRNA		

Table 3.3.1.2: Contact sites with tRNA phosphates at the P site that were strongly protected in two different elongator tRNAs, namely $tRNA^{Phe}$ and $tRNA^{Met}$. nt, nucleotidyl residue; aa, aminoacyl residue; Eubact., eubacterial domain; 3 domains, the eubacterial, archeal and eubacterial domains

Only one example with a 80-90% conserved base in bacteria is in the position 1909 of 23S rRNA (less than 80% conservation in three domains). Furthermore, we identified a number of conserved aminoacyl-positions of ribosomal proteins that neighbor these phosphates. For example, position 120 (*E. coli* numbering) of S13 is always a Lys or an Arg residue and lies next to tRNA base G30, a highly conserved Arg128 of S9 protein neighbors tRNA base Y32 and positions Arg/Lys56 and Arg/Lys64 of L5 are in close proximity to C56. An example of the alignment is given in Figure 3.3.1.2 with the

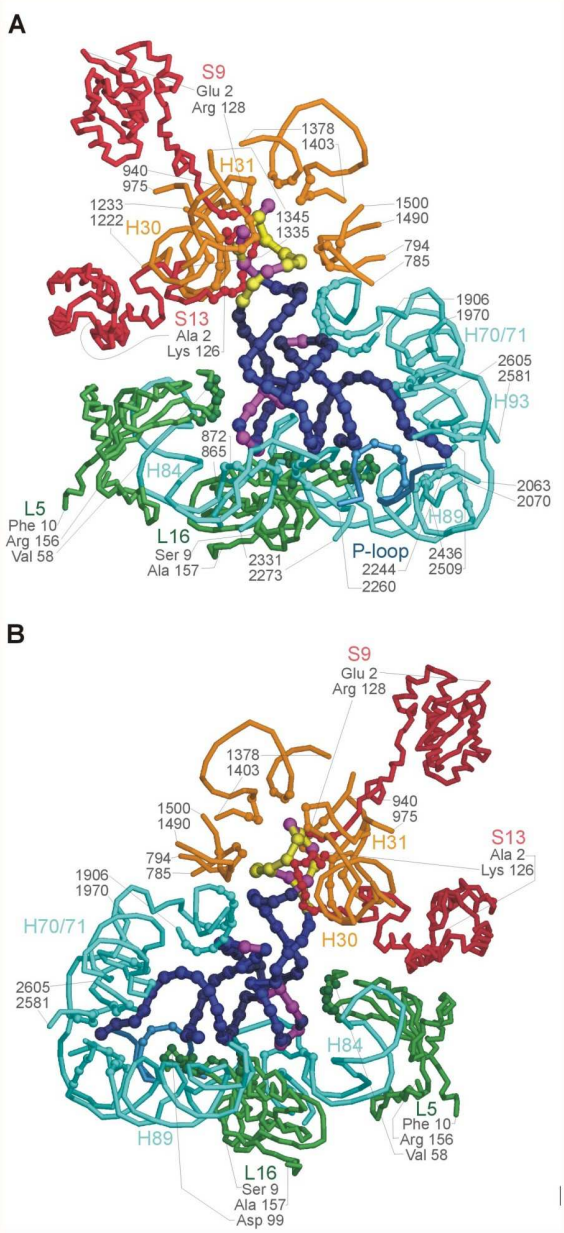

Figure 3.3.1.1: tRNA neighborhoods at the ribosomal P site of the 70S ribosome according to ((Yusupov et al., 2001), see also Table 3.3.1.2). A, view from the A site; B, view from the E site. tRNA: yellow, contacts with the small subunit; blue, contacts with the large subunit; pink, strongly protected sites in both tRNA ^{Phe} and $tRNA_m^{Met}$ at the P site. Regions of the ribosomal components that are within a 10 Å radius of the P-site tRNA are indicated with spheres. 30S components: gold, 16S rRNA; red, S-proteins. 50S components: cyan, 23S rRNA; green, L-proteins.

ribosomal protein S9. Besides the approximately 90% conserved Arg128 residue, Ser126 and Lys127 with 50% conservation lie next to the tRNA base Y32.

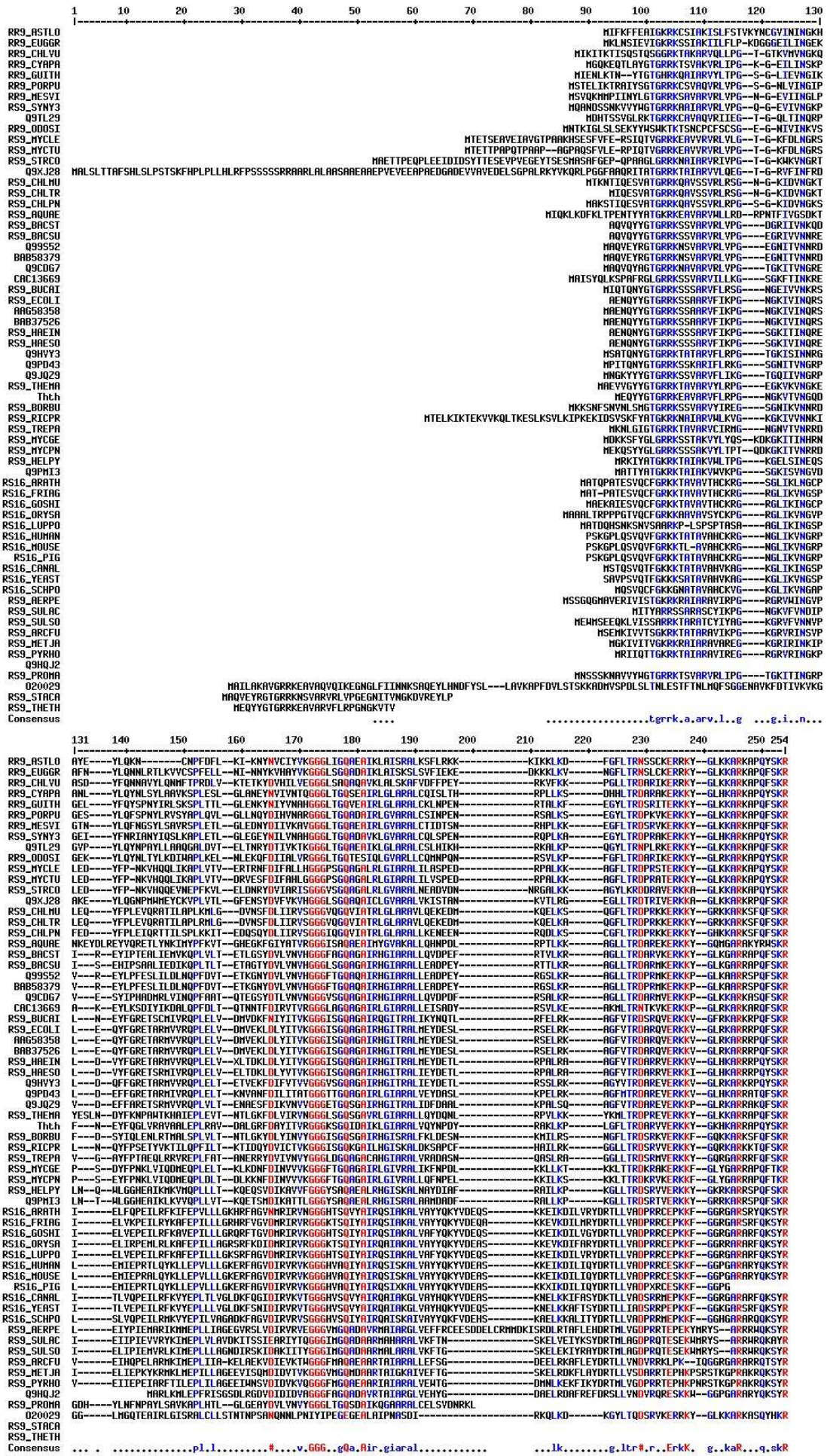

Figure 3.3.1.2: Example to the alignment of ribosomal protein S9. Left are the organisms listed. Red, universally conserved residues; blue, highly conserved residues. The residues Arg128 (*E. coli* nomenclature) and the preceding semi-protected Lys127 and Ser126 are shown in residues 252-254 in the Figure.

3.3.2 tRNA protections seen with isolated 30S and 50S subunits can be added to the protection pattern found in the P site of programmed 70S ribosomes

Thioated $tRNA^{Phe}$ was bound to 30S and 50S subunits and the respective protection patterns generated were compared with that for the P site of complete programmed 70S (Schäfer, 1997; Schäfer et al., 2002). Strikingly, the results show that the region 30±1 to 43±1 is protected in 30S subunits and 70S ribosomes in an almost identical fashion, whereas the regions outside this sequence are clearly less protected in the 30S subunits. A complementary picture was found when the protection pattern in the 50S subunit was compared with that of the 70S ribosome, i.e. no correspondence of protections between sequences 29 to 43, instead a good agreement outside of this region. Here, we wanted to compare Schäfer's results with the recently available 5.5 Å map of the tRNA·70S complex. We used the Ras-Mol program for analysis and transferred the script files to the Pov-Ray for preparing the figure. According to our analysis, the contribution of each subunit to the overall distribution of contacts made with the P site tRNA is in remarkable concordance with the 5.5 Å map of the tRNA·70S complex (see Table 3 in ref. (Yusupov et al., 2001)) and also with the mimic of an anticodon-stem loop structure in the crystal of 30S subunit (Carter et al., 2000). In Figure 3.3.2.1 we illustrate that Schäfer's footprinting data is in excellent agreement with the 5.5 Å map of a 70S complex The 30S protections of the anticodon stem-loop structure (positions 30±1 to 41±1 in blue) are located exclusively in the neighborhood of 30S components (green and blue) of the 70S map, whereas the remaining portion of the tRNA (dark red) lies within the domain of the 50S subunits (yellow and orange).

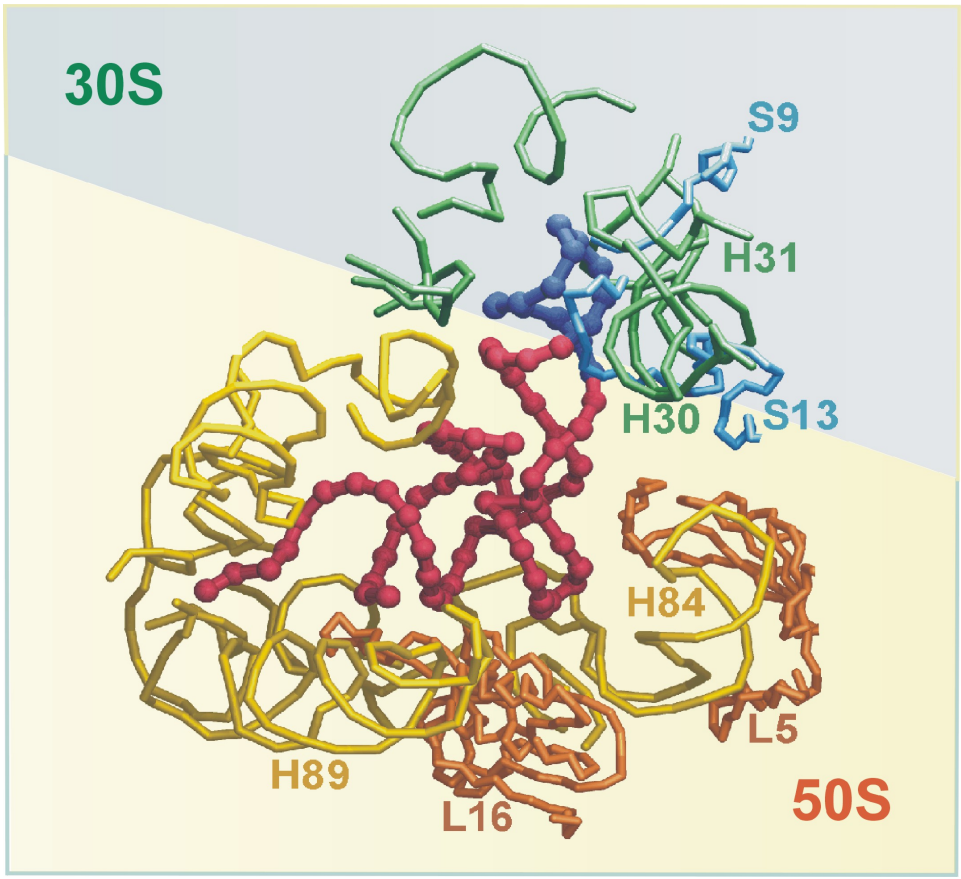

Figure 3.3.2.1: Delineation of the tRNA on the 70S and 30S and 50S subunits. For details see text.